SHEAR STRENGTH OF PANELS

Fumitoshi Ishikawa

A Dissertation

in the

Centre for Building Studies

Presented in Partial Fulfillment of the Requirements for the Degree of Master of Engineering (Building) at Concordia University, Montreal, Quebec, Canada.

September 1981

ABSTRACT

Abstract

SHEAR STRENGTH OF PANELS

Fumitoshi Ishikawa

A plate girder consists of flanges (top, bottom), a plate for the web with stiffeners (vertical and/or longitudinal). The mechanical properties of the parts are not necessarily the same. The capacity of such a girder, subjected to shear force and moment, may be limited by the buckling of the web. The complexity of the behaviour of the web after buckling makes the prediction of the ultimate strength quite difficult. Wagner's theoretical model [9], composed of a web in diagonal tension with strong flanges was the first applied for post-buckled webs. A number of researchers have proposed various stress models [1] for predicting the ultimate strength. Most of the models have been semi-empirically defined, but none of them takes care of the stresses at the boundaries. Thus each stress model predicts the ultimate strength for girders of proportions within specific ranges for the size and properties of the component.

In the present study, a single square panel, stiffened with uniform flanges along all the edges, is considered as one special case for plate girders. By taking a single panel, rather than a whole plate girder, and applying shear force only along the edges, the parameters considered for the plate girders are considerably reduced without loss of generality and a

clearer picture up to the ultimate capacity of the plate girder can be shown by the experiment. Actual stress distribution and ultimate strength of the panels depend on how the panels are arranged, but the fundamental stress distribution in the web remains the same for any type of panel.

The analysis of the experiments examines mainly how the stress distribution changes at each load and how it differs from the theory.

ACKNOWLEDGEMENTS

ACKNOWLEDGES

I would like to express my sincere thanks to Prof. Cedric Marsh, my supervisor and advisor, who directed me through my studies.

National Science and Engineering Research Council of Canada, which provided financing, and the Centre for Building Studies which provided facilities for the studies, are also acknowledged.

Additional thanks are due to Mr. J. Zilka and Mr. O. Hans, lab technicians, who aided me on numerous occasions during the experiments. Mrs. Susan Regan and Ms. Catherine Nishimura are also thanked for typing my thesis.

TABLE OF CONTENTS

TABLE OF CONTENTS

TABLE OF CONTENTS (cont)

LIST OF FIGURES

LIST OF FIGURES

LIST OF FIGURES (cont.)

LIST OF TABLES

LIST OF TABLES

NOTATIONS

NOTATION

a, b = panel dimensions

A_w = area of web

b_f = breadth of flange

c = distance from corner to plastic hinge in flange

e = $g - c$

e' = $b - c$

C = a factor

g = length of normal tension zone on flange

M = bending moment

M_o = plastic moment of resistance of flange

s = length of yield zone in shear at boundary of web

s' = length which would replace length s, influenced by flange strength

t, t_f = thicknesses of web and flange

V = shear force supported by web

V_{cr} = initial buckling shear force

V' = shear force supported by flange

V_u = ultimate shear force

x, y = co-ordinates

X_B = distance along a boundary

α = g/b

β = e/g

β' = $\frac{e'}{b}$

μ = $M_o/b^2 t\, \tau_y$

σ_b = maximum bending stress

σ_{bc} = critical bending stress

σ_t, σ_c = tensile and compressive normal stresses

NOTATION

σ_y = yield stress of webs

τ_{yf} = yield stress of flanges

τ_{xy} = shear stress

τ_y = yield stress in shear

τ_{yf} = yield stress in shear of web

τ_c = shear stress for initial buckling

τ_o = minimum shear stress at collapse

τ_e = mean shear stress contributed by web

τ_e' = mean shear stress contributed by flange

CHAPTER 1

Introduction

Chapter 1

INTRODUCTION

In the past five decades, work on shear post-buckling behaviour of stiffened webs of plate girders has been carried out experimentally and analytically by a number of researchers.[1] These studies have been directed towards the design of girders used in Civil structures and Aircraft.

A survey of stress models used in the analysis of diagonal tension webs is given in [1]. Each of the models, however, fails in some way to satisfy the essential requirements of the stress system, either normal to the boundaries where the tension stress is not balanced, or in the distribution of stress along the boundaries. Those models satisfy only overall equilibrium of the girder.

In Chapter 2, the stress field defined by Marsh, based on an entirely different assumption from any other previous models, is introduced. That stress field satisfies the equilibrium conditions without normal stress acting at the boundaries, except as a limiting state. A rational picture of the limiting structural behaviour is presented by dividing the shear capacity of the girder into that contributed by the web and that contributed by the flange.

In Fig. 1-1, three stages of the collapse modes of girders are shown. As the flange strength increases, other dimensions remaining constant, the collapse modes change from that in (a) to that in (c), which represents the extreme case. These collapse modes are also referred to in the earlier models of diagonal tension field.

In 1929, Wagner [9] established "the theory of complete tension field." As shown in Fig. 1-2, he assumed that a pure shear stress system exists before buckling of a web and it changes to a uniaxial stress system in tension after buckling of the web. He showed that the tensile stress runs at an inclination of 45°. His theory can be applied only for plate girders having a skin-like web with rigid flanges. Such a type of plate girder can be found in aircraft such as in a wing spar. A collapse mode of a plate girder described above, whose flange strength enables it to carry the load due to full normal stresses occurring along the boundaries, is shown in Fig. 1-1 (c).

In 1963, Basler [2] assumed an imcomplete tension field, shown in Fig. 1-3. For a post-buckled web, this stress system would apply to the plate girder flanges having a low strength.

There are two differences in this assumption

compared to Wagner's theory. One is that compressive stress orthogonal to the tension field remains even after the buckling of the web. The other, which is in the major difference, is that the tension field is not reacted by the flanges. The assumption about the stress system after buckling can be considered as a superposition of the two types of stress, the buckling stress (τ_{cr}) and the tension stress (σ_t), as shown in Fig. 1-3. The plate girder with flanges so flexible where no normal stress could exist along the boundaries would yield a collapse mode, shown in Fig. 1-1(a).

Although both theories described above may give good approximations in ultimate skin strength for the girders having extreme flange strength, they are not applicable to plate girders used in Civil Engineering which possess flange strengths lying between the extremes and yield a collapse mode, as shown in Fig. 1-1(b).

Rockey and Skaloud [5] presented the tension field whose angle is equal to the inclination of the geometrical diagonal with a tension field symmetric with respect to this diagonal, shown in Fig. 1-4(a). The width of the diagonal tension field is assumed to be such that at its junction with the flange its edges coincide with the position of the plastic hinges in the flanges. The position of the plastic

hinges in the flanges is assumed to be related to the flange stiffness parameter, I_f/b^3t. They showed that the plastic hinge approaches, but does not pass the half the flange length.

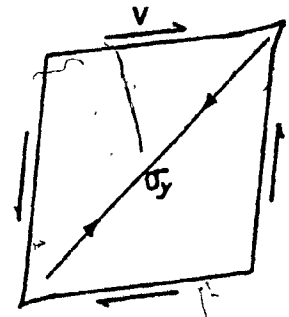

(a) Collapse Mode with No Flange Strength (Mp=0)

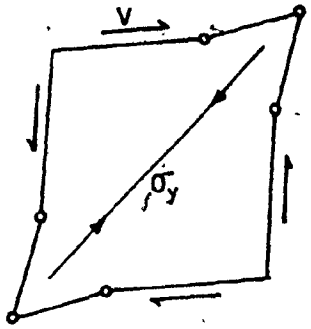

(b) Collapse Mode with Medium Flange Strength (Mp=medium)

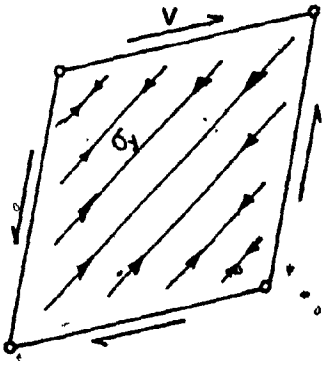

(c) Collapse Mode with High Flange Strength (Mp=high)

FIG. 1.1 COLLAPSE MODES OF PANELS

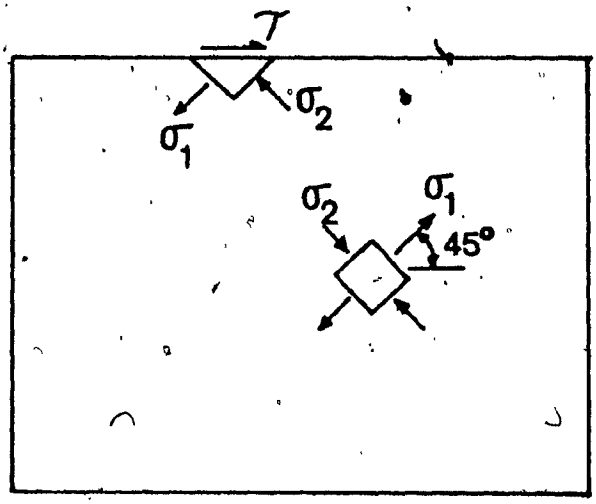

(a) Pure Shear Stress System

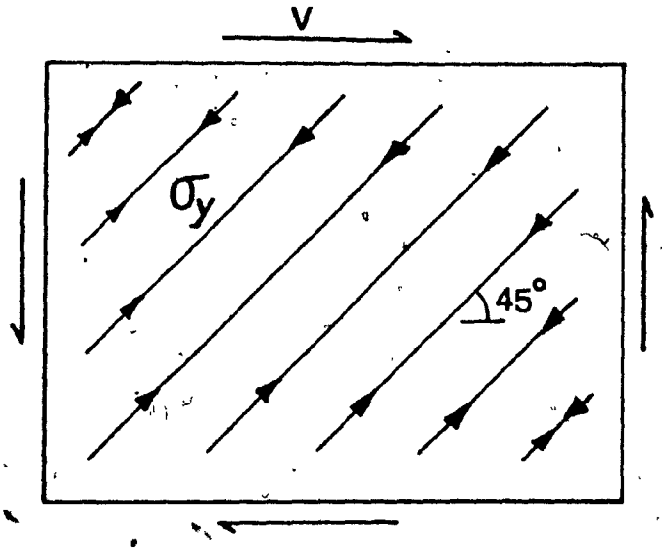

(b) Diagonal Tension Field

FIG. 1.2 COMPLETE DIAGONAL TENSION FIELD

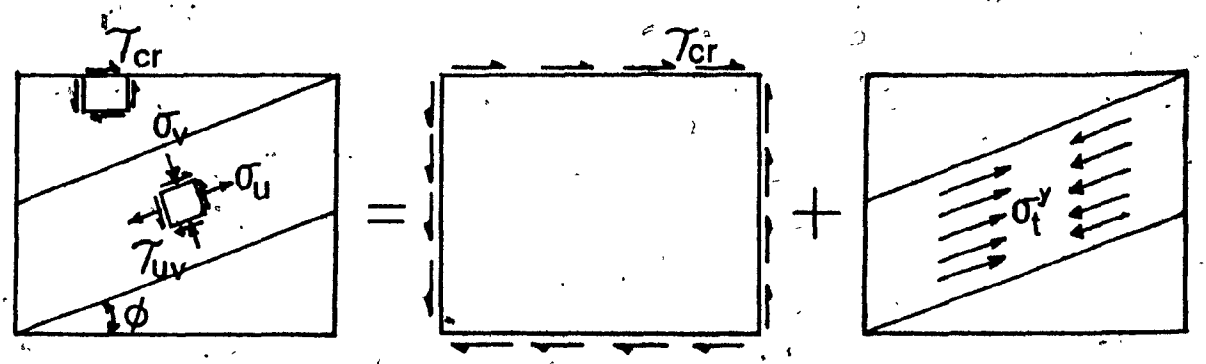

(a) Collanse Mode (b) Critical Mode (c) Membrane Stress Field

FIG. 1.3 ULTIMATE LOAD MECHANISM

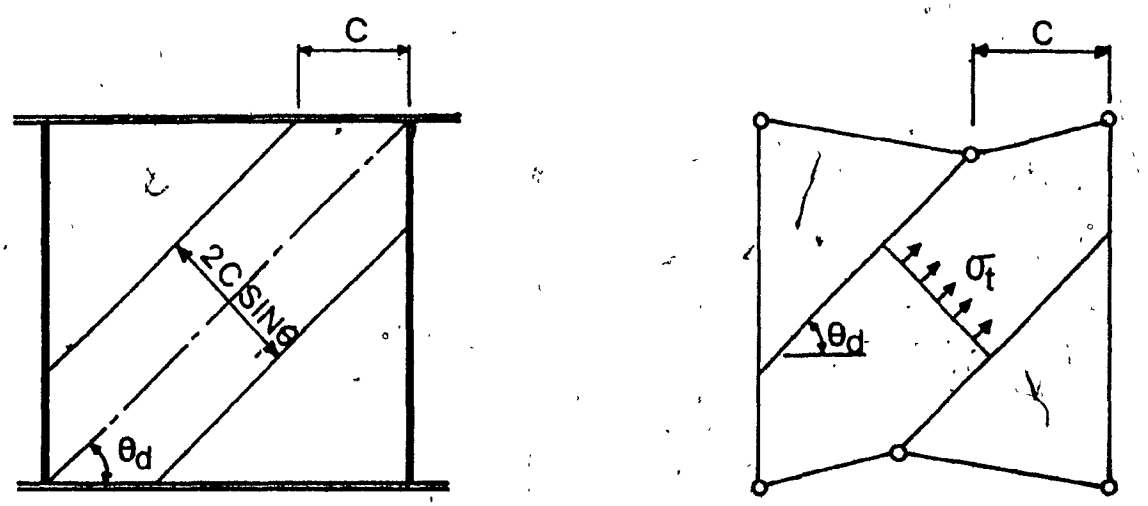

(a) Inclination of Diagonal Tension Field (b) Beam Mechanism with Plastic Hinges

FIG. 1.4 BEAM MECHANISM ASSUMED AT ULTIMATE LOAD

CHAPTER 2

Theory

CHAPTER 2

THEORY

2.1 The Development of the Theory

The shear panel considered in the present theory is square with uniform stiffening flanges along the edges.

The flanges are integrally attached to the web of the panel but are initially assumed to possess no independent flexural rigidity in the plane of the web.

If this panel is subjected to a shear force, it is evident that there can be no normal stress at right angles to the boundaries, thus a state of shear stress with, possibly, normal stress parallel to the boundaries, must exist immediately adjacent to the boundary stiffeners.

After initial buckling at a uniform shear stress, as the load increases the shorter diagonals can accept higher stresses, and the final condition approaches a series of

diagonal strips buckling in compression.

The shear stress, which can be resolved into tension and compression components as in Fig. 2-1, is assumed to vary in a manner dictated by the compression component. This component is limited to an elastic buckling stress which is taken to be inversely proportional to the square of the length of the line AB, and is expressed as:

$$(1)\quad \sigma_c = \tau_o \left(\frac{b}{x_B}\right)^2$$

in which σ_c = compression stress, x_B = distance from the corner to the point B, τ_o = initial buckling stress.

At the boundary:

$$(2)\quad \sigma_c = \sigma_t = \tau_{xy}$$

in which τ_{xy} = shear stress.

If the stress along any line running at 45^o is assumed to remain constant, then at any point in the web the stresses are given by:

$$(3)\quad \tau_c = \tau_o \left(\frac{b}{x+y}\right)^2 \leq \tau_y$$

$$(4)\quad \sigma_t = \tau_o \left(\frac{b}{x-y}\right)^2 \leq \tau_y$$

for values of $(x + y) < b$, b = length of one side.

At any point in the region $(x + y) < b$ the vertical shear stress is then:

$$(5)\quad \tau_{xy} = \frac{\tau_o b^2}{2} \left[\frac{1}{(x+y)^2} + \frac{1}{(x-y)^2}\right]$$

This stress has a maximum value of τ_y which in turn

limits σ_c and σ_t to τ_y, where τ_y is the yield stress of the web in shear.

The extent of the yield zone in the corner (Fig. 2-2) is given by:

$$(6)\quad \sigma_c = \tau_o\left(\frac{b}{x+y}\right)^2 = \tau_y \quad , \quad \sigma_t = \tau_o\left(\frac{b}{x-y}\right)^2 = \tau_y$$

leading to:

$$(6.a)\quad \text{compression}: (x+y) = b\left(\frac{\tau_o}{\tau_y}\right)^{\frac{1}{2}} = s$$

$$(6.b)\quad \text{tension}: (x-y) = b\left(\frac{\tau_o}{\tau_y}\right)^{\frac{1}{2}} = s$$

It is to be observed that the limiting stress is the shear yield adjacent to the corner of the panel; the diagonal tension stress remote from the corners remains elastic, representing a condition prior to the observed limit (Rockey, 1968).

Equilibrium requires that the shear force, V, be balanced across all orthogonal sections by the sum of the shear fluxes:

$$(7)\quad V = t\int_o^b \tau_{xy}\, dx$$

Along the edge, at y = o, this becomes:

$$V = t\int_o^s \tau_y\, dx + t\int_o^b \tau_o\left(\frac{b}{x}\right)^2 dx$$

Using equation (6), leads to:

$$(8)\quad V = bt[2(\tau_o\tau_y)^{\frac{1}{2}} - \tau_o]$$

It can be shown that this value is constant for all sections.

In expression (8), although τ_o is an elastic shear buckling stress as stated before, it will be influenced by the proportion of the panels, by the presence of compressive stresses due to overall bending, and by the torsional stiffness of the flange.

After initial buckling, there is no reason to assume that the compression stress along the main diagonal will remain constant as post-buckling deformation develops, or that τ_o is necessarily related to the initial buckling stress.

However, for the present study, in order to satisfy continuity of the design expressions, τ_o is taken to be initial critical stress.

Expression (8) can then be written in the form:

$$(9)\quad \tau_e/\tau_y = V/bt\tau_y = 2(\tau_o/\tau_y)^{\frac{1}{2}} - \tau_o/\tau_y$$

where τ_e = the equivalent shear stress = V/bt

The initial critical stress is given by:

$$(10)\quad \tau_o = 5.75\left(1 + 0.75\left(\frac{b}{a}\right)^2\right)\frac{\pi^2 E}{12(1-\nu^2)}\left(\frac{t}{b}\right)^2$$

in which a = panel length, b = panel width.

To take account of the influence of the bending stress in the plane of the web, the critical shear stress is multiplied by: $\left(1 - \left(\frac{\sigma_b}{\sigma_{bc}}\right)^2\right)^{\frac{1}{2}}$

σ_b = maximum axial stress in the flange

σ_{bc} = critical for in-plane bending stresses in the web.

An optimum plate girder section has a flange area of about half the web area, thus, if the end panel is square, the bending stress is about double the shear stress. Expression (10) for a square panel becomes approximately:

$$(11)\quad \tau_o \gtrsim 7E\left(\frac{t}{b}\right)^2$$

2.2 Influence of the Flange Strength

The flange modifies the shear capacity by:

(a) its influence on the edge fixity;

(b) its influence on the ratio of the bending stress to the shear stress;

(c) its bending strength.

Only the last influence is of interest.

At first glance it would appear that the flange cannot act as a beam independently of the web to which it is attached and that any bending resistance it possesses must involve at least part of the web. However, the web is not capable of carrying any increase in shear stress that would be demanded by the combined action of the web and flange in bending. It follows that an increase in the diagonal tension component can only be reacted by shear force across the flange area itself, causing the flange to bend without

assistance from the collapsed web. The additional tension is carried as a component normal to the flange. The stress changes from that represented by the Mohr's circle in Fig. 2-3(1) to that of Fig. 2-3(2). The second system represents diagonal tension.

For simplicity the Tresca yield condition is used, i.e. $\sigma_y = 2\tau_y$

a) The Additional Shear Force due to the Bending of the Flange: The additional shear, V', is transferred from the web to the flange by tension stress with a maximum value of $\sigma_y/2$ in the corner, and is assumed to reduce linearly to zero at a distance, g, from the corner (Fig. 2-4(a)).

A plastic moment, Mo, occurs at a distance, c, from the corner. As the moment must be a maximum at C, the shear force there is zero. Using a triangular distribution of normal stress, the following relationships can be established:

Let $\alpha = g/b$, $\beta = (g-c)/b$ (see Fig. 2-4(a))

For $\alpha < 1$.

The location of the plastic hinge is found by moment equilibrium at the hinge.

$$R_1 = \frac{\tau_y t}{2} \frac{e^2}{g}$$

$$R_2 = \frac{\tau_y t}{2g} (g^2 - e^2)$$

$$\frac{\tau_y t}{2g}(g-e)^3 + \frac{\tau_y t}{6g} e^3 = \frac{\tau_y t}{2g} e^2(b - g + e)$$

$$+ \frac{2\tau_y t}{2x3g}(g-e)^3 + \frac{\tau_y t}{2g} e(g-e)^2$$

$$g^3 = 3be^2$$

$$(\frac{e}{b})^2 = \frac{1}{3}(\frac{g}{b})^3$$

(12) $\beta = \alpha(\frac{\alpha}{3})^{\frac{1}{2}}$

The contribution to the shear capacity is:

$$V' = R_2 - R_1$$

(13) $\tau_e'/\tau_y = \alpha(1 - 2\alpha/3)/2$

where $\tau_e' = \frac{V'}{bt\tau_y}$

The relationship between plastic moment, Mo, in the flange and the length of the normal tension zone, is

(14) $\mu = \frac{\alpha^2}{6} [1 - \alpha(1 - 2\alpha/3\sqrt{3})]$

in which $\mu = \Sigma Mo/b^2 t\tau_y$

For $\alpha > 1$ (see Fig. 2-4(b)).

β is obtained from the equation

(15) $\beta'^2/2\alpha + \beta'(1 - 1/\alpha) - (1/2 - 1/3\alpha) = 0$

where $\beta' = \frac{e'}{b} = \frac{e - (g-b)}{b} = (b-c)/b$

The contribution to the shear capacity is then:

(16) $\tau_e'/\tau_y = 1/6\alpha$

The relationship between μ , α, and β is:

$$(17)\quad \mu = [(1 - 2/3\alpha)\beta' - \beta'^2(1 - 1/\alpha) - \beta'^3/3\alpha]/4$$

It is to be observed that when

$$\mu = 1/16\ ,\ \tau'_e/\tau_y = 0$$

This represents the Wagner stress system in which the flange behaves as rigid and the web is at the limit of its capacity.

With a further increase in the strength of the flanges the behaviour changes to that of a tension web inside a frame. If the corner connections between the flanges in the square panel are pinned, the web strength limits the capacity. If the connections are rigid, or the flanges are continuous, such that the plastic moment can be developed at the corners, the flanges and stiffeners form a frame capable of carrying additional shear.

As the flange strength increases, the distance C to the plastic hinge increases and the additional shear force contributed by the flanges is given by:

For $1/16 < \mu \leq 1/4$, i.e. $c < b$

$$(18)\quad \tau'_e/\tau_y = 4\mu^{\frac{1}{2}} - 1$$

For $\mu > 1/4$ i.e. $c = b$

$$(19)\quad \tau'_e/\tau_y = 4\mu$$

The final condition for the square panel with a rigid frame is shown in Fig. 5, in which the shear capacity is the sum of that which causes the yielding of the web in tension and that which causes the plastic yielding of the frame, acting as a Vierendeel truss.

Fig. 2-8 gives the relationship between τ'_e/τ_y and $\mu = \frac{Mo}{b^2 t \tau_y}$ for the complete range of behaviour as Mo increases from zero.

The value of α is determined by μ, but it is not readily extracted from equations (14) and (17), so this relationship is also plotted in Fig. 2-7.

If the flange is not continuous, and only a single hinge is formed, Mo is replaced by Mo/2. This will only be valid up to $\mu = 1/16$, beyond which there will be no frame action to carry a higher shear force.

b) <u>The influence of the Flange Strength on Shear Capacity of the Web</u>: The flange contributes to the total shear capacity of the panel by virtue of its bending strength. In addition, the tension normal to the flange increases the shear stress in the web for values of $g > S$, i.e. if the tension zone is longer than the zone of shear yielding at the web/flange interface. This occurs when $\alpha > (\tau_o/\tau_y)^{\frac{1}{2}}$, where $\alpha = g/b$

The stress normal to the boundary is assumed to be $\tau_y(1 - x/g)$, (Fig. 2-4).

Assuming that the compression component remains constant, the shear stress at the boundary becomes:

$$(20)\quad \tau_{xy} = \tau_o(b/x)^2 + \tau_y(1 - x/g) \geq \tau_y$$

The length which yields in shear is thereby increased to:

$$(21)\quad s' = b(\alpha\tau_o/\tau_y)^{1/3}$$

Along the boundary the total shear force is then:

$$V' = s't\tau_y + \int_{s'}^{b} t\,\tau_o(b/x)^2 dx + \int_{s'}^{g} t\,\tau_y(1-x/g)dx$$

For $(\tau_o/\tau_y)^{1/2} < \alpha < 1$, (Fig. 4(a)), this gives:

$$(22)\quad \tau_e/\tau_y = \frac{3}{2\alpha}(\alpha\frac{\tau_o}{\tau_y})^{2/3} + \frac{\alpha}{2} - \frac{\tau_o}{\tau_y}$$

For $\alpha > 1$, (Fig. 4(b)), this expression becomes:

$$(23)\quad \tau_e/\tau_y = \frac{3}{2\alpha}(\alpha\frac{\tau_o}{\tau_y})^{2/3} + 1 - \frac{1}{2\alpha} - \frac{\tau_o}{\tau_y}$$

and when $\alpha \geq \tau_y/\tau_o$:

$$\tau_e/\tau_y = 1$$

which is the Wagner stress system for the web.

The shear capacity of the web, V, is thus determined by τ_o/τ_y and α, which is determined by $\mu = Mo/b^2t\tau_y$

Fig. 2-7 gives the relationship between τ_e/τ_y and μ for various values of τ_o/τ_y.

Fig. 2-6 illustrates the two components of the stress system in the web, at the limit, for values of $\mu \leq 1/16$.

Total Capacity

The shear contributions due to the web and the flange, which depend on the values of τ_e/τ_y and $\mu = \frac{Mo}{b^2 t \tau_y}$, are shown in Fig. 2-7 and is also given in Table 2.1 showing the equations defined previously.

To compute the shear capacity of a panel the procedure is:

Calculate τ_o/τ_y and $\mu = Mo/b^2 t\tau_y$

In Fig. 2-7, where the value of μ intersects the curve for τ_o/τ_y gives the value of τ_e/τ_y on the ordinate;

Where the value of μ intersects the curve for τ'_e/τ_y gives the value of τ'_e/τ_y on the ordinate:

The total shear capacity is then:

$$(24)\quad V + V' = (\tau_e/\tau_y + \tau'_e/\tau_y)\, bt\tau_y$$

TABLE 2.1

Summary of the Equations

μ	α	τ_e/τ_y Shear contribution due to web	τ_e'/τ_y Shear contribution due to flange
0	0	$\frac{\tau_e}{\tau_y} = 2\left(\frac{\tau_o}{\tau_y}\right)^{\frac{1}{2}} - \frac{\tau_o}{\tau_y}$	$\frac{\tau_e'}{\tau_y} = 0$
$\mu < 1/16$	$\alpha < \left(\frac{\tau_o}{\tau_y}\right)^{\frac{1}{2}}$	$\frac{\tau_e}{\tau_y} = 2\left(\frac{\tau_o}{\tau_y}\right)^{\frac{1}{2}} - \frac{\tau_o}{\tau_y}$	$\frac{\tau_e'}{\tau_y} = \frac{\alpha}{2}\left(1 - \frac{2\alpha}{3}\right)$
	$\left(\frac{\tau_o}{\tau_y}\right)^{\frac{1}{2}} < \alpha < 1$	$\frac{\tau_e}{\tau_y} = \frac{3}{2\alpha}\left(\alpha\frac{\tau_o}{\tau_y}\right)^{2/3} + \frac{\alpha}{2} - \frac{\tau_o}{\tau_y}$	
	$\alpha > 1$	$\frac{\tau_e}{\tau_y} = \frac{3}{2\alpha}\left(\alpha\frac{\tau_o}{\tau_y}\right)^{2/3} + 1 - \frac{1}{2\alpha} - \frac{\tau_o}{\tau_y}$	$\frac{\tau_e'}{\tau_y} = \frac{1}{6\alpha}$
	$\alpha \geq \frac{\tau_y}{\tau_o}$	$\frac{\tau_e}{\tau_y} = 1$	
1/16	∞		$\frac{\tau_e'}{\tau_y} = 0$

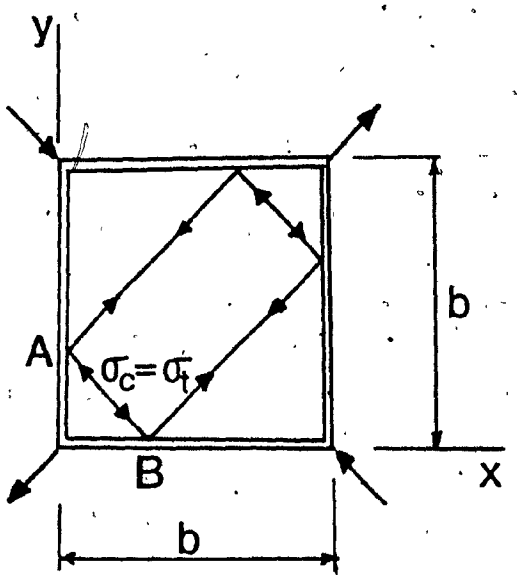

FIG. 2-1 STRESSES IN SHEAR PANEL

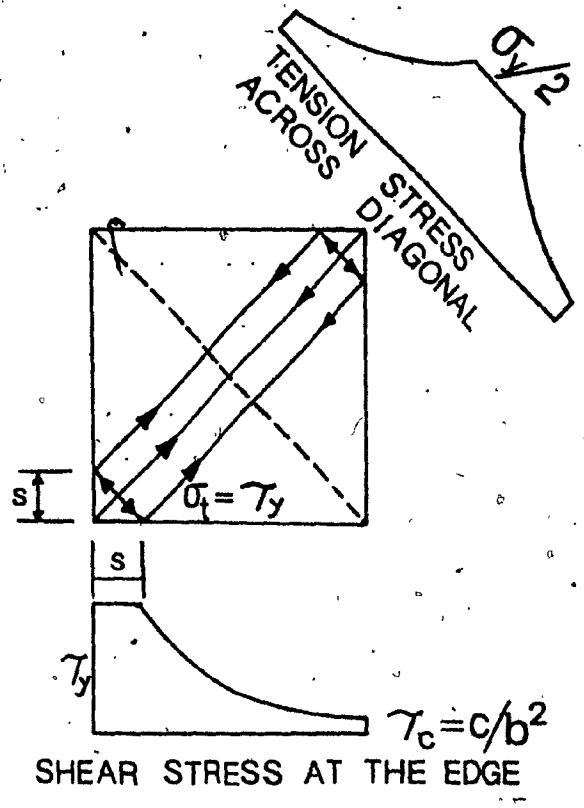

FIG. 2-2 SHEAR AND TENSION DISTRIBUTION

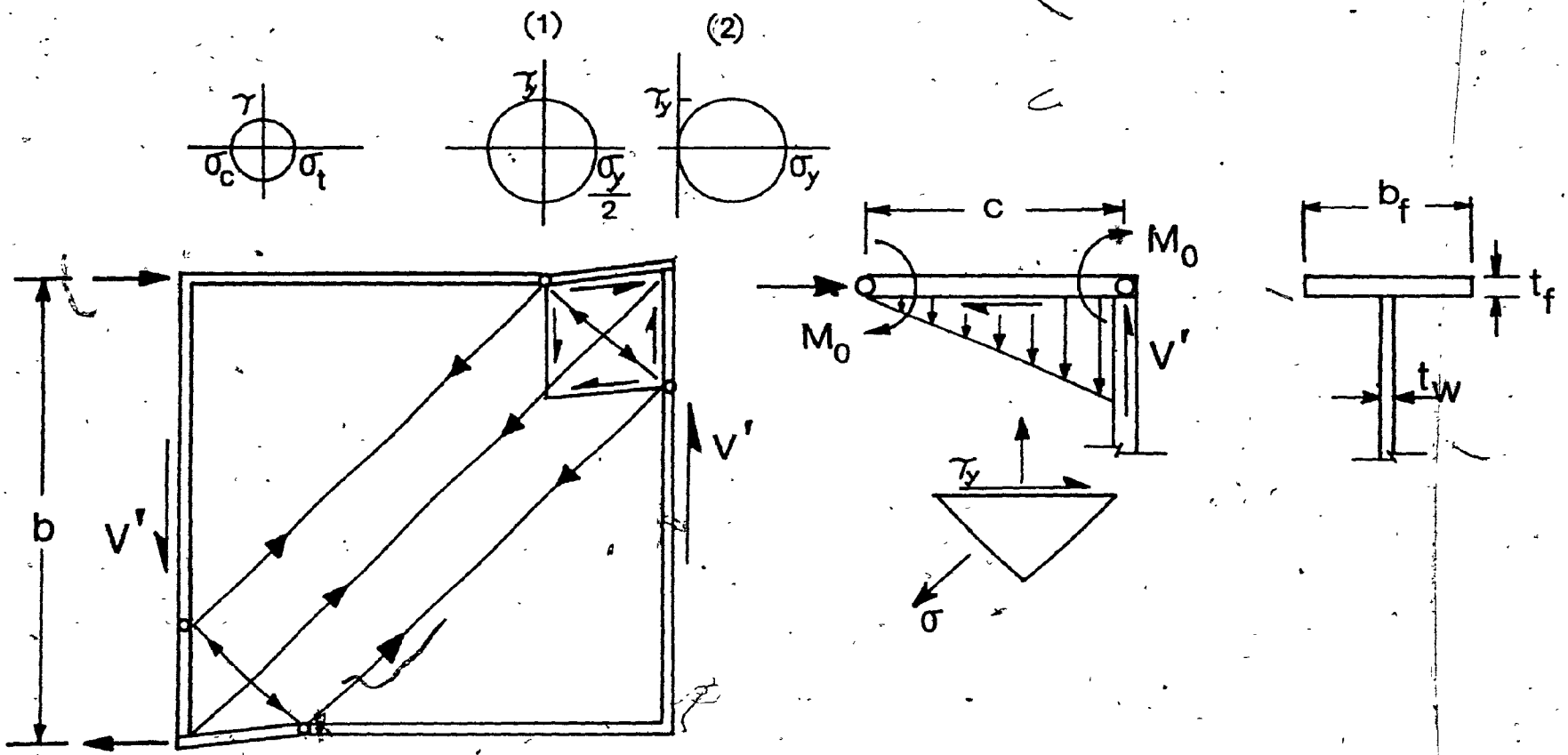

FIG. 2-3 STRESS SYSTEM AT THE BOUNDARY

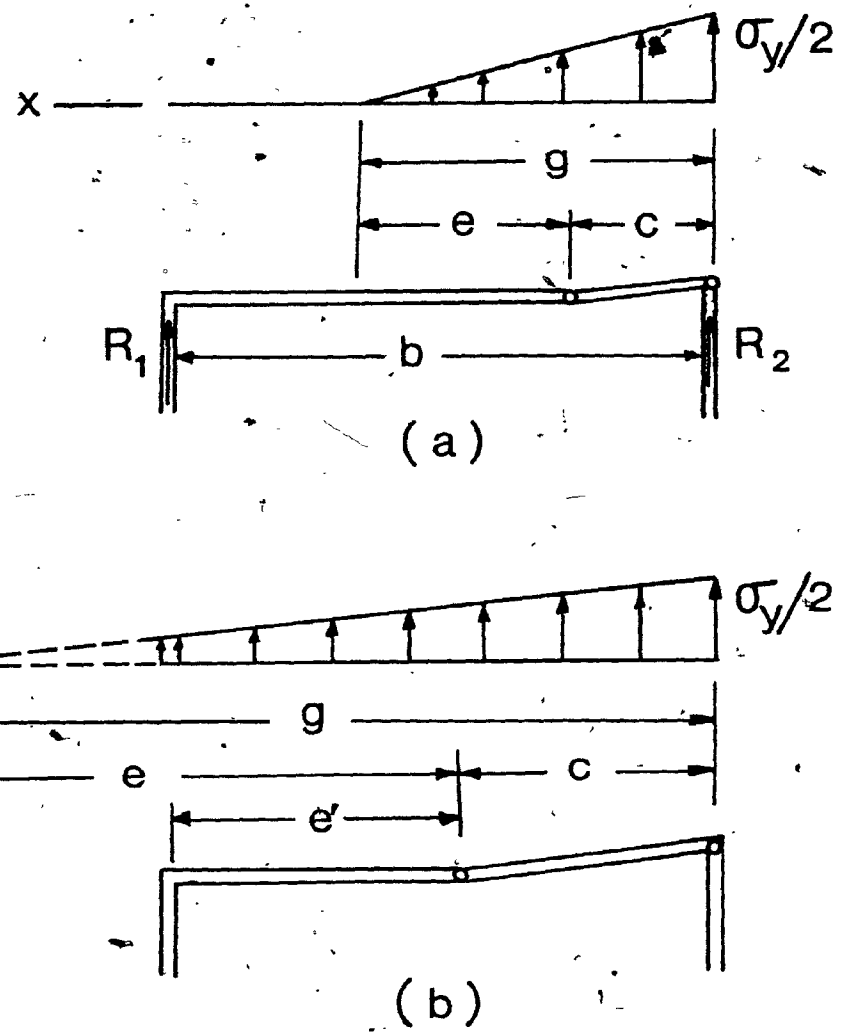

FIG. 2-4 DISTRIBUTION OF NORMAL TENSION STRESS AND LOCATION OF PLASTIC HINGES IN THE FLANGE

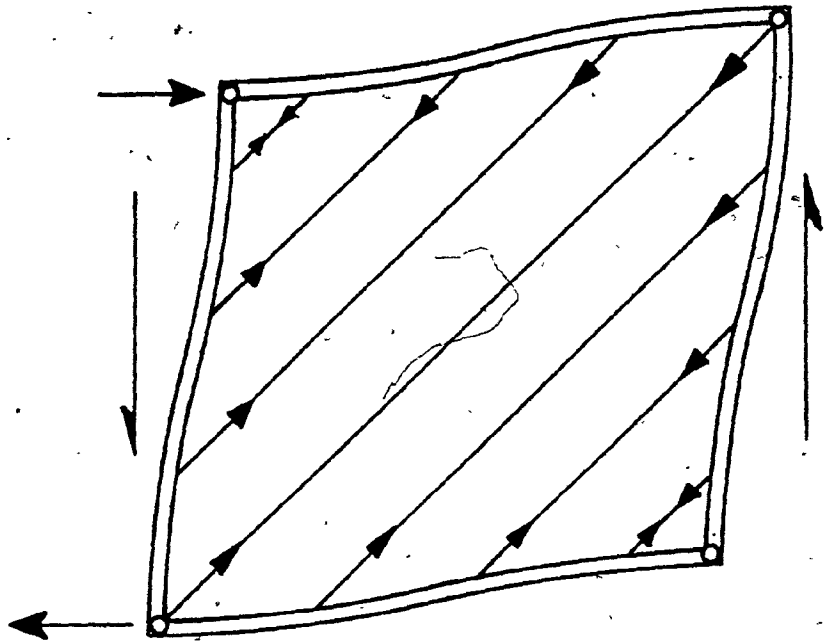

LIMIT CONDITION OF STIFFENED SHEAR WEB

FIG. 2-5 LIMIT CONDITION OF YIELDED WEB AND FLANGE FOR $\mu \geq \frac{1}{4}$

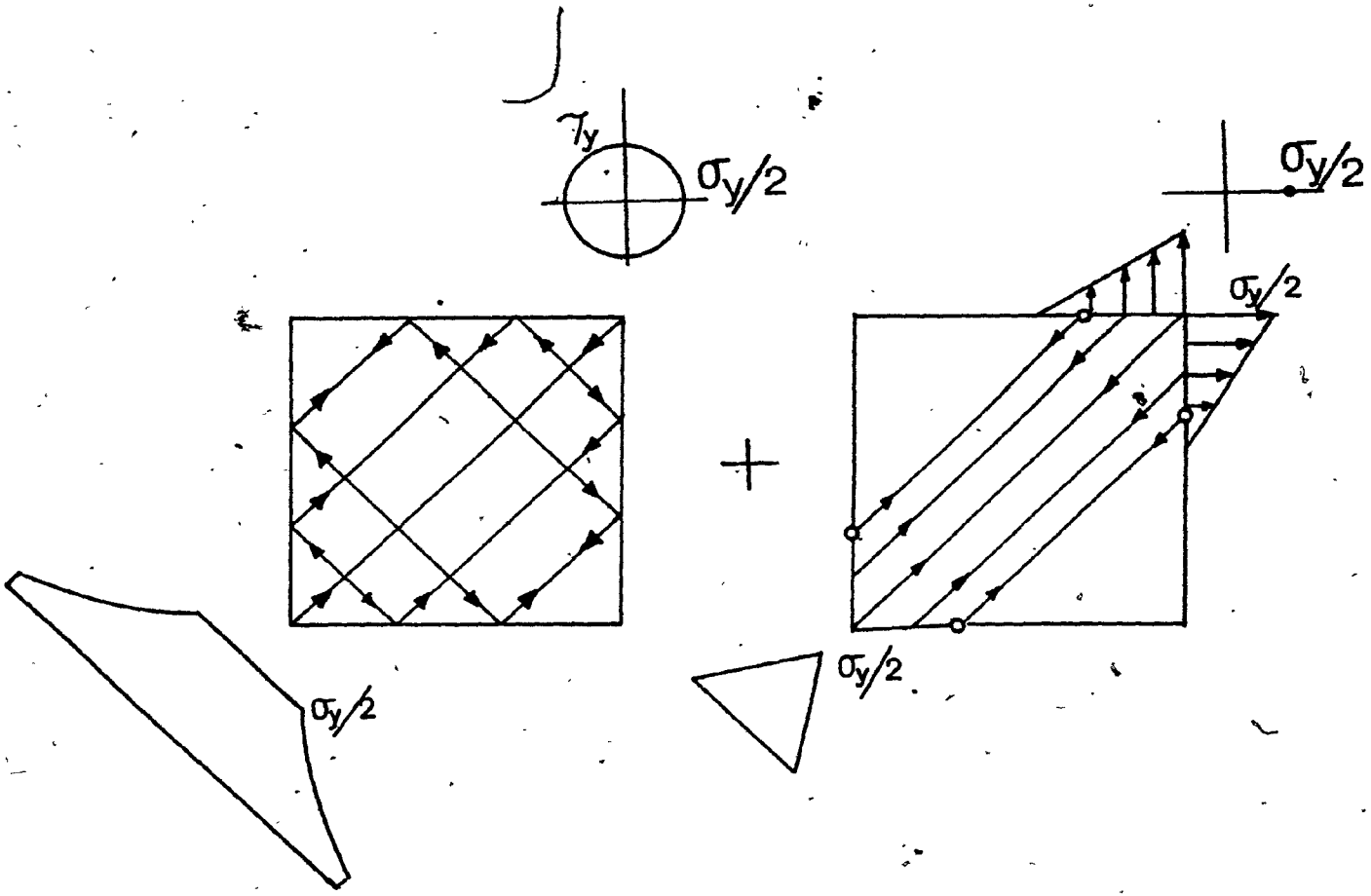

Shear Resistant Component

Diagonal Tension Component

(The Mohr's circles indicate the stress at the corner)

FIG. 2-6 LIMITING STRESS SYSTEM IN THE WEB FOR $\mu > 1/16$

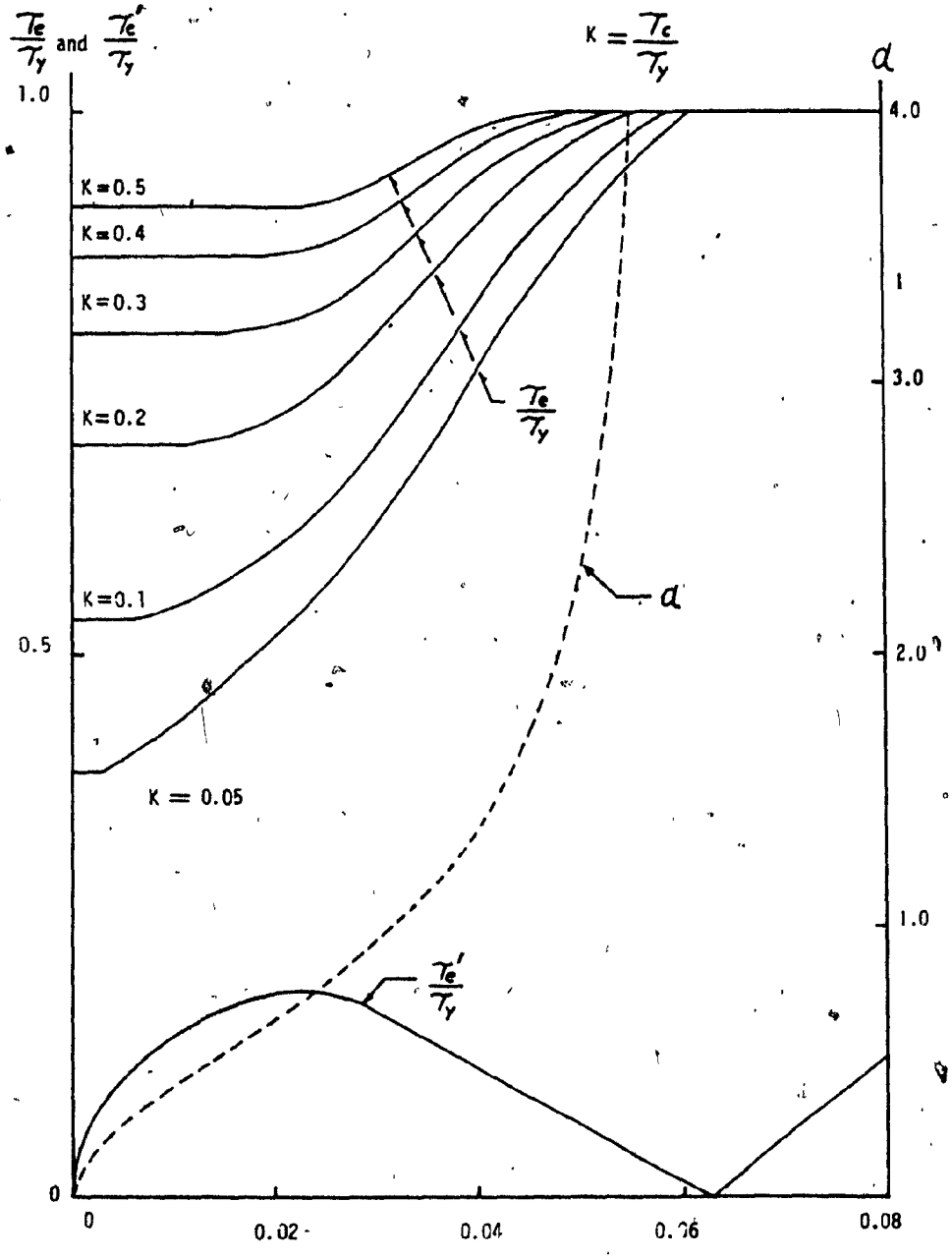

FIG. 2.7 CURVES TO DETERMINE COLLAPSE LOAD

CHAPTER 3

Experiments on Panels with Flanges Subjected to Shear Force

The gauge locations, and some notations which are used in Chapters 3 and 4, are shown in Fig. 3.1.

A number of experiments to determine the ultimate strength of shear panels, with or without longitudinal stiffners, have been carried out in the past as shown in (1). Usually plate girder type specimens, in which shear force and moment are combined, have been tested. This has complicated the analysis and the comparison with the theory.

The aim of the experiments in this study was that the panels be subjected to shear force only. Tests were conducted on two single-panel specimens to see the correlation between the experiment and the theoretical values, such as stress distribution in the web, and the initial buckling and ultimate strengths of the panels.

3.1 Description of Test Panels

For the experiments of the present study the following test panel specimens were prepared. They were square and stiffened by uniform flanges all around the edges (as shown in Fig. 3.2 and Fig. 3.3 (a) and (b)). Ratio of breadth (b) and thickness (t) of the webs, denoted as b/t, was taken high enough so as to let the web buckle at a low shear stress compared with shear yielding. The panels were instrumented to measure stress distribution along the edge before and after the

web buckles.

In Table 3.1 the dimension of the panels and the yield strengths of the steels used for the webs and the flanges are shown. It is to be mentioned that the steel used for the web of the panel No. 2 had quite a low yield strength, 32 ksi, but this was not a factor in the testing or in the analysis of the results. The flanges and the webs were welded together along all the edges of the webs, as can be seen in Fig. 3. There were six holes in each flange for the bolts to apply the load in Test 1. The loading system is described more fully in section 3.3.

3.2 Measurements in Testing Panels

3.2.1 Membrane Strain

It is important to know how the stresses in the panels are distributed, and how they change in the pre- and post-buckling of the panels.

To obtain the stress distribution, rossette gauges (3-element 45° rectangular rossette) were used on both faces of the web in order to get membrane strain. This meant that each pair of rossette gauges, on opposite faces, had to be placed exactly at the same place in the same direction as shown in Fig. 3.1.

3.2.2 Out-of-Plane Deformation of the Panels

Out-of-plane deformation of the panels was measured at each loading using a device with a dial gauge (1/1,000 inches)

shown in Fig. 3.7. The data obtained from readings gave the initial deformation and the change of deformation modes of the panels with the increase of the load. The effect of the initial deformation on the initial buckling was examined from these measurements.

White wash was also used on one face of the web so that initial yielding and progress of the buckling up to the ultimate capacity of the panel could be clearly observed.

3.3 Methods of Loading

Two different methods of loading were used. For the panel specimen No. 1, two steel loading brackets, shown in Fig. 3.4, were connected to the flanges by the bolts in an attempt to transfer the loading to the web by shear force along the edge. The bolts passed through the holes in the bracket and the flanges, but were not tightened, so that the bracket could slide in the direction normal to the edge to avoid force across the edge. The bolts used in this experiment were high strength, heavy structural bolts, A490.

For the specimen No. 2, a compression was directly applied to the corners of the specimen as shown in Fig. 3.6(b). This method of the loading was used since the method of the loading for the specimen No. 1 showned that there were forces acting normal to the edges.

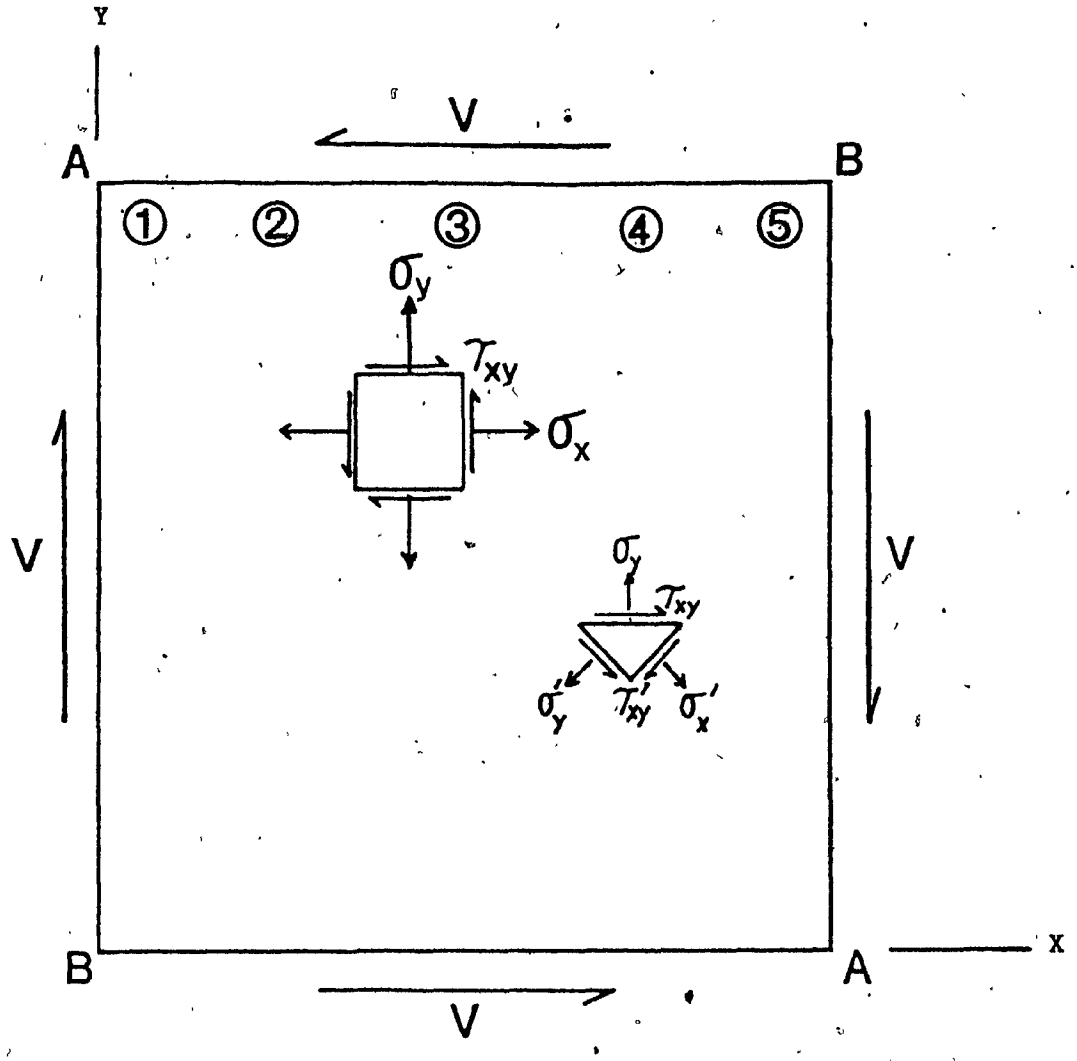

FIG. 3-1 NOTATIONS USED IN CHAPTERS 3 AND 4

Note:

1) V = applied shear force at the edges

2) The numbers in the circles along the edge are "gauge number"

3) All stresses acting on the elements have positive sense

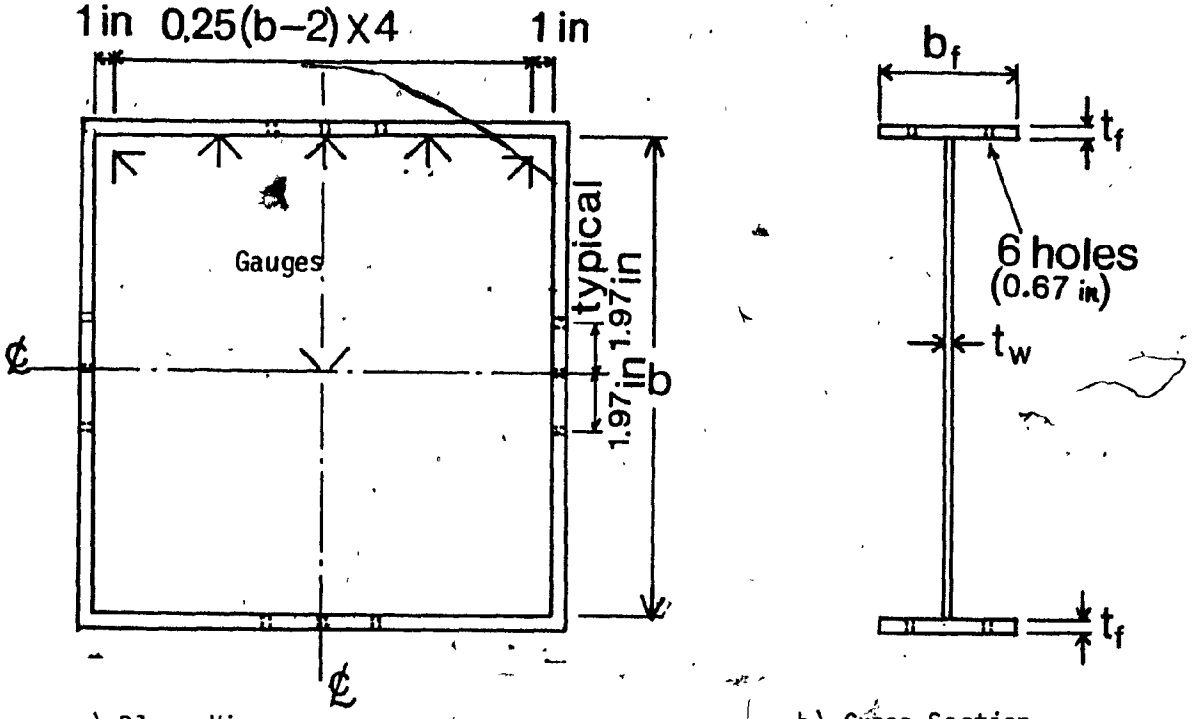

FIG. 3.2 Experimental Shear Panel

specimen number		1	2
b (in)		15.23	15.05
t_w (in)		0.081	0.125
b_f (in)		3.91	3.946
t_f (in)		0.25	0.327
σ_y (ksi)	(flange)	58.23	48.94
	(web)	51.93	31.94

TABLE 3.1 SIZE AND YIELD STRENGTHS OF PANEL SPECIMENS

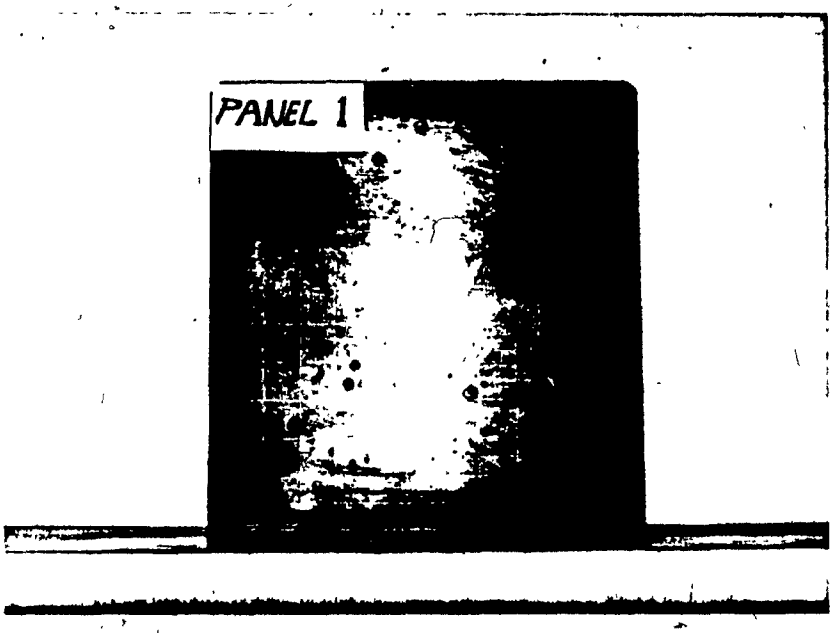

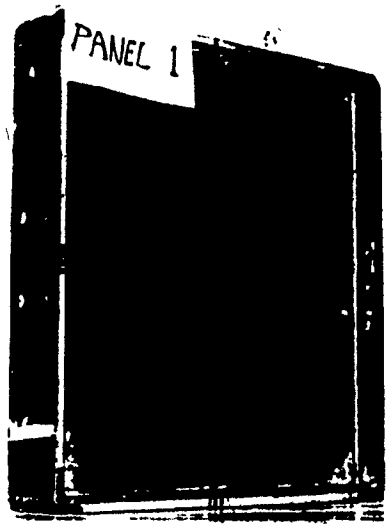

FIG. 3.3 (a) PANEL SPECIMEN 1 BEFORE TESTING

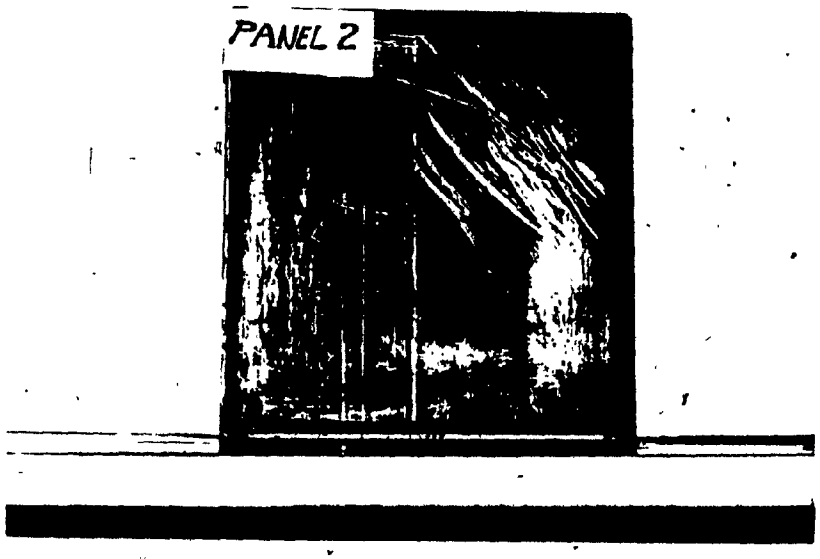

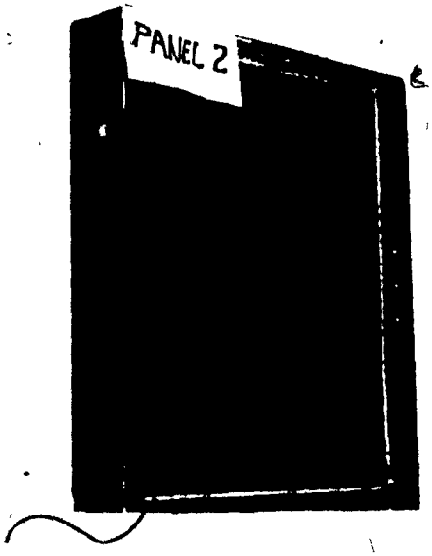

FIG. 3.3. (b) PANEL SPECIMEN 2 BEFORE TESTING

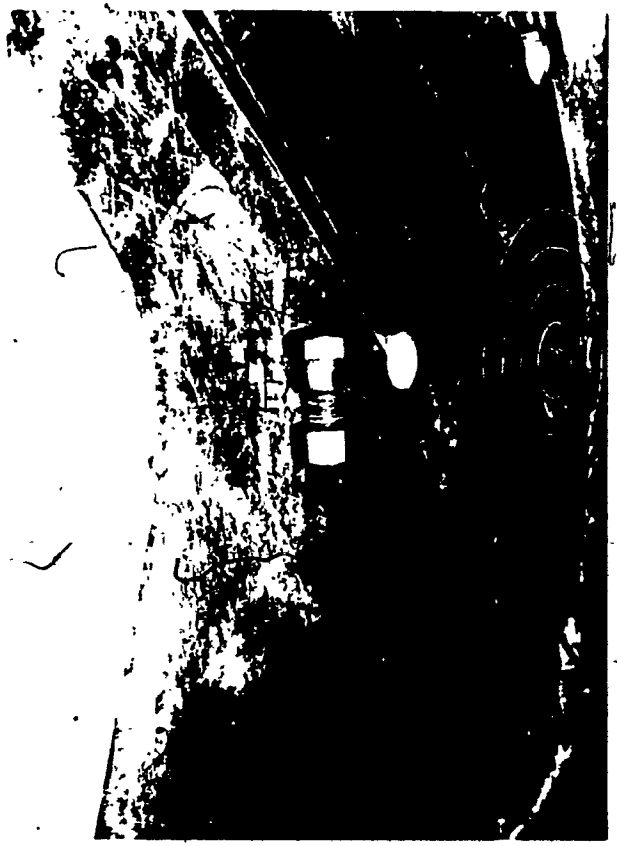

FIG. 3.5 BOLTS (A 490; DIAMETER = 5/8 INCHES)

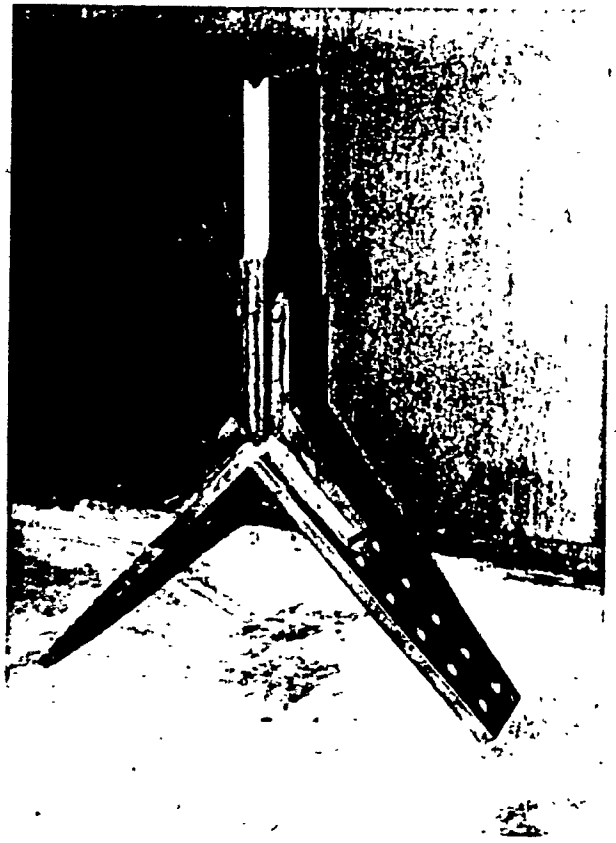

FIG. 3.4 LOADING BRACKET USED FOR THE PANEL NUMBER 1

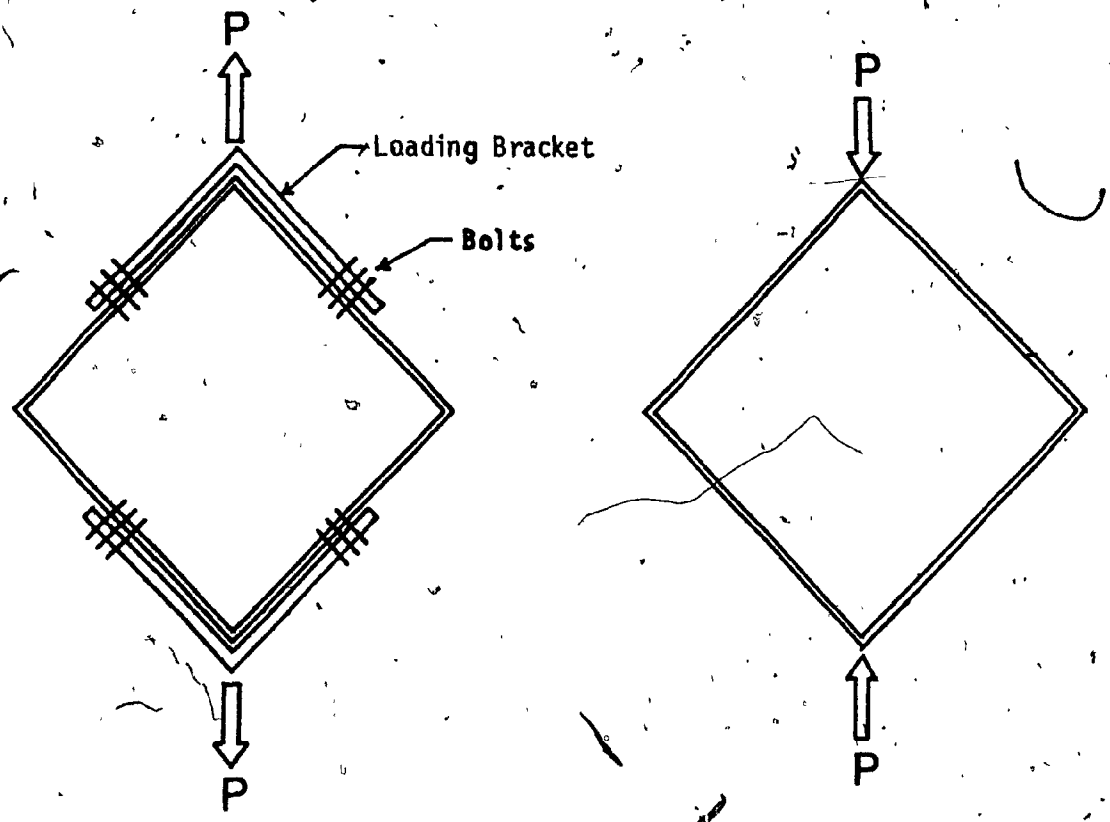

a) Panel Number 1 b) Panel Number 2

FIG. 3.6 LOADING SYSTEM

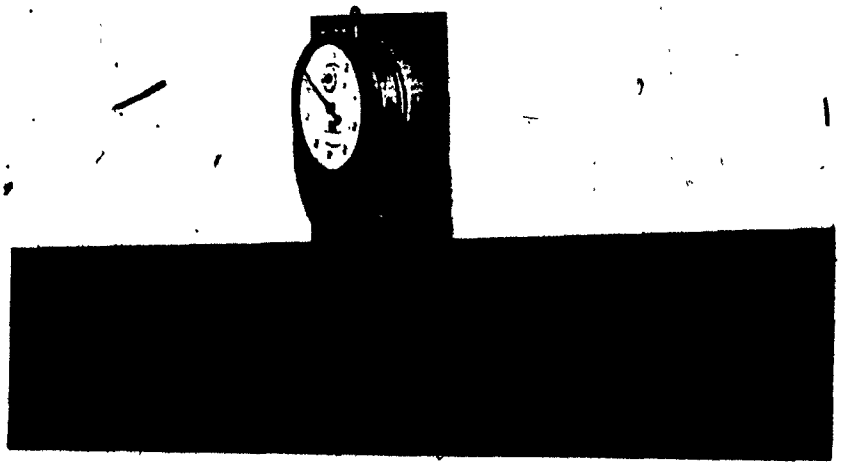

FIG. 3.7 THE DEVICE TO MEASURE OUT-OF-PLANE DEFORMATION OF THE WEBS

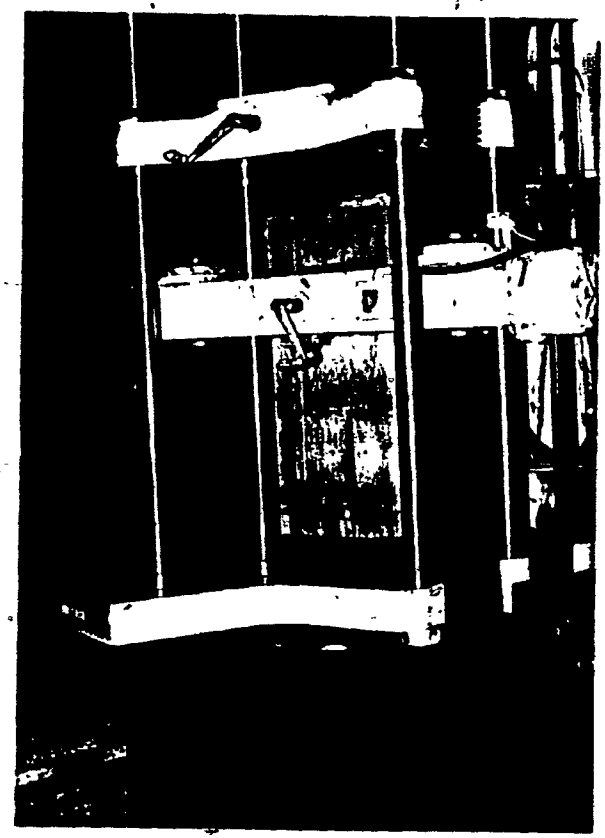

FIG. 3.9 LOADING MACHINE(TENIUS OLSEN)

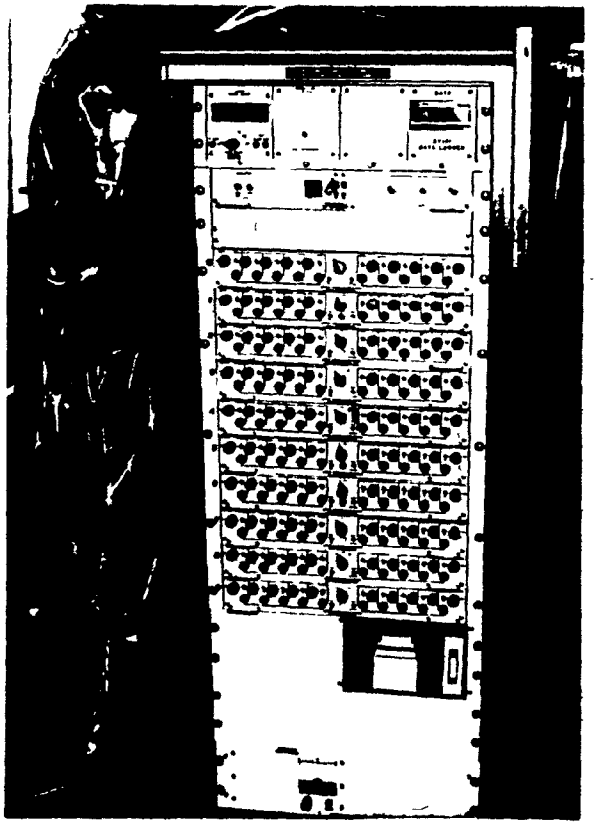

FIG. 3.8 DIGITAL DATA ACQUISITION SYSTEM

CHAPTER 4

Experiment Results and Discussion

CHAPTER 4

Experiment Results and Discussion

In the experiments on the two panels, strain measurements were made to determine the shear stress along the edge, stresses normal to the edge (called "normal stress"), initial buckling stress, ultimate strength, ultimate deformation and position of plastic hinges.

First it is to be noticed that the shear (see Fig. 4.1(a) and (b)) and normal stress (see Fig. 4.2(a) and (b)) patterns for the panels No. 1 and No. 2 are quite different. This is attributed to the different manners of loading.

4.1 Results and Discussion of Panel No. 1

4.1.1. Correlation of Shear and Normal Stresses along the Edge: Panel No. 1

As was shown in Chapter 3, the load in shear was applied in the direction from the corner B to the corner A (see Figure 3.1 and 4.1(a) for stresses).

As shown in Fig. 4.2(a) for the specimen No. 1, there are locally non-negligible stresses normal to the edge. Those could be due to either 1) tensile force in the bolts or 2) moment created by the eccentric load at the bolts, or 3) both of them.

The tensile force in the bolts could be caused by engagement of the bolt threads not permitting the sliding anticipated while the moment would be due to the gap between the flange and

the loading bracket.

The force acting normal to the edge, calculated from the normal stress in Fig. 4.2(a), approximately summed up to zero, so the stress system is self-equilibrating. This means that cause 2) mentioned above is more likely. This would also suggest that the load must have been carried by the shear force only along the edge at least up to the load of 45 kips. The moment induced at the position of the bolts also influenced this shear distribution shown in Fig. 4.1(a). This moment was created between the gauge numbers 2 and 3 (see Fig. 4.2(a)). The values of the shear stress at gauge number 2 is always lower than the ones at gauge number 3. If the influence due to this moment is considered, the shear stress shown in Fig. 4.1(a) up to the load of 25 kips is reasonably uniformly distributed from gauge numbers 1 to 4. while the shear stress at gauge number 5 remained low, as anticipated. The stress at gauge number 1 as collapse was approached was lower than at gauge 2. This is explained by the local influence of the loading arrangement. At the load 45 kips, the stress pattern can be approximated by a bilinear form. The shear stresses at the gauge numbers 1, 2 and 3 have reached yield and the stresses between the gauge numbers 3, 4 and 5 change almost linearly. This stress pattern differs from the present theory which assumes changing quadratically in the region that has not yielded.

The stress at the corner B remained at less than half the buckling stress.

Summarizing the results of the shear and the normal stresses along the edge for the panel number 1, it will follow that:

1) There are non-negligible normal stresses which are self-equilibrating. This was due to the moment induced by the eccentric load of the bolts.
2) From 1) it is clear that the load was carried only by the shear along the edge until the load of 45 kips.
3) The shear stress pattern can be approximated by a bilinear form.
4) At the load 45 kips, the stress at the gauge numbers 1, 2 and 3 had passed the yield while the stress at the gauge number 5 remained small.
5) The normal stress at the corner A remained zero until the load of 45 kips. The normal stress at the corner B was small.

The summary of the results concludes as follows;

1) Discounting the normal stress discussed in 1) normal stress required to form plastic hinges in the flanges was not detected by the gauges.

   This fact means that the tension diagonal field (normal stress along the edge), commonly studied in the past work, is not developed immediately after buckling.
2) The conclusion 1) supports the relevance of an assumption used in the present theory which says that a shear stress system along the edge remains until it reaches yield in the corner, and then the additional shear is

carried by the flange whose rigidity causes normal stress along the edge.

3) As was implied in the result 3), the shear stress pattern at the load, representing the maximum shear stress capacity of the web itself, is of a bilinear form rather than the one assumed in the present theory.

4.1.2 The Collapse and the Ultimate Strength of the Panel No.1

At collapse, as seen in Fig. 4.3(a), plastic hinges were formed in the flanges, at the corner A_1 only. This lack of symmetry was due to the action of the loading brackets.

The position of the plastic hinges in the experiment is 3.75 inches from the corner while the theoretical one is 3.13 inches. That is very close considering the secondary effect of the loading system.

The ultimate shear strength of the panel in the experiment was 53 kips while the theoretical is 30 kips which is the sum of 25.5 kips, shear capacity of the web only and 4.5 kips, contributed by the flanges. The experimental result is 78% higher than the theoretical one. The reason is difficult to establish as strain readings were abandoned after 45 kips, but from the action of the specimen it is assumed that tension stress was transferred directly across the web between loading points.

The shear stress distribution is shown in Fig. 4.1(a). It is seen that the experimental results is always higher than the values of $P/bt\sqrt{2}$. Sums of the shear fluxes to give the total shear forces, calculated from Fig. 4.1(a), are 15% to 20% lower

than the applied shear forces. To be sure, the sums of the stress fluxes in the direction of the load were also calculated and they were were also 10% to 20% lower than the applied load. Those errors are assumed to be experimental.

4.2 Results and Discussion of the Panel No. 2

4.2.1. The Correlation of the Shear and the Normal Stresses along the Edge

First it can be noticed that the stresses at the corner B, shown in Fig. 4.1(b) and 4.2(b), were locally influenced by the load directly applied at the corners, and this influence will be considered in the following discussion.

In the early stage of loading up to 30 kips, ignoring the stresses locally influenced at the corner B, the shear stresses (Fig. 4.1(b)) are fairly uniform and the normal stresses are negligibly small. As the load increases from 30 to 40 kips, which is after the buckling load of 36 kips, the shear and the normal stress distributions changed. The shear stresses at the gauge numbers 1 and 2 nearly doubled, while yielding at gauge number 5 has already occured due to the load being applied at that corner. The shear stress at the gauge number 1 was always lower than that at gauge number 2, as happened to the panel number 1.

The distribution of normal stress (Fig. 4.2(b)) at the load of 40 kips, after buckling occured, varies from compression at the gauge numbers 1 and 2, to tension at the gauge numbers 3 and 4. The normal stresses are almost self-cancelling

and seem to arise from the action of the flange to compression at gauge 5. The normal stress at the corner A remained zero. It follows that the load was carried by shear only along the edge up to the load of 40 kips and the shear capacity of the web had not yet been reached.

Summarizing the results discussed above, it will follow that:

1) The shear stresses (Fig. 4.1(b)) are initially uniform, ignoring the gauge number 5 where yielding occurred due to the load being applied directly at the corners,
2) There were negligibly small normal stresses along the edge implying that the web carried only shear.
3) Clear distribution of the normal stress was formed when the load reached to 40 kips. This was due to the deformation of the edge which would have changed the shear flow. However, the stress is self-cancelling and as is seen from the zero normal stress at the corner A (Fig. 4.2(b)), the load in shear was still carried by the web.

4.2.2 The Collapse and the Ultimate Strength of the Panel No. 1

As can be seen from Fig. 4.3(b), the plastic hinges occured in the flanges at both the corners A_1 and A_2, but they were all formed at the bolt holes. The position of these bolts was 5 inches from the corners compared to the theoretical location of the plastic hinge of 3.2 inches.

The ultimate shear strength in the experiment was 30.4 kips ($=43/\sqrt{2}$) while the theoretical one is 38.9 kips which is the sum of 34.1 kips, for the capacity of the web only and 4.8 kips, contributed by the flanges. The 21% lower value for the experimental result was assumed to be due to the loading system and the bolt holes.

Finally it can be noticed that the sums of the fluxes to give the total shear forces, calculated from Fig. 4.2(a), is 10% to 30% lower than the applied shear. The error is due to the load being applied at the corner such that some portion is carried directly by the flanges and some is radially distributed into the web.

Table 4.1
Summary of Shear Panel Tests on Single Panels

Specimen Number	V_{cr} exp	V_{cr}th	V_u exp	V_{th}		V_uth	C exp	C_{th}	A_w
				Web	Flange				
1	26.9	7.1	53.	25.5	4.5	30	3.8	3.1	1.25
2	25.5	24.4	30.4	34.1	4.8	38.9	5.0	3.6	1.88

Note: exp ... Experimental values
th ... Theoretical values

* The units used are in kips, inches and square inches.

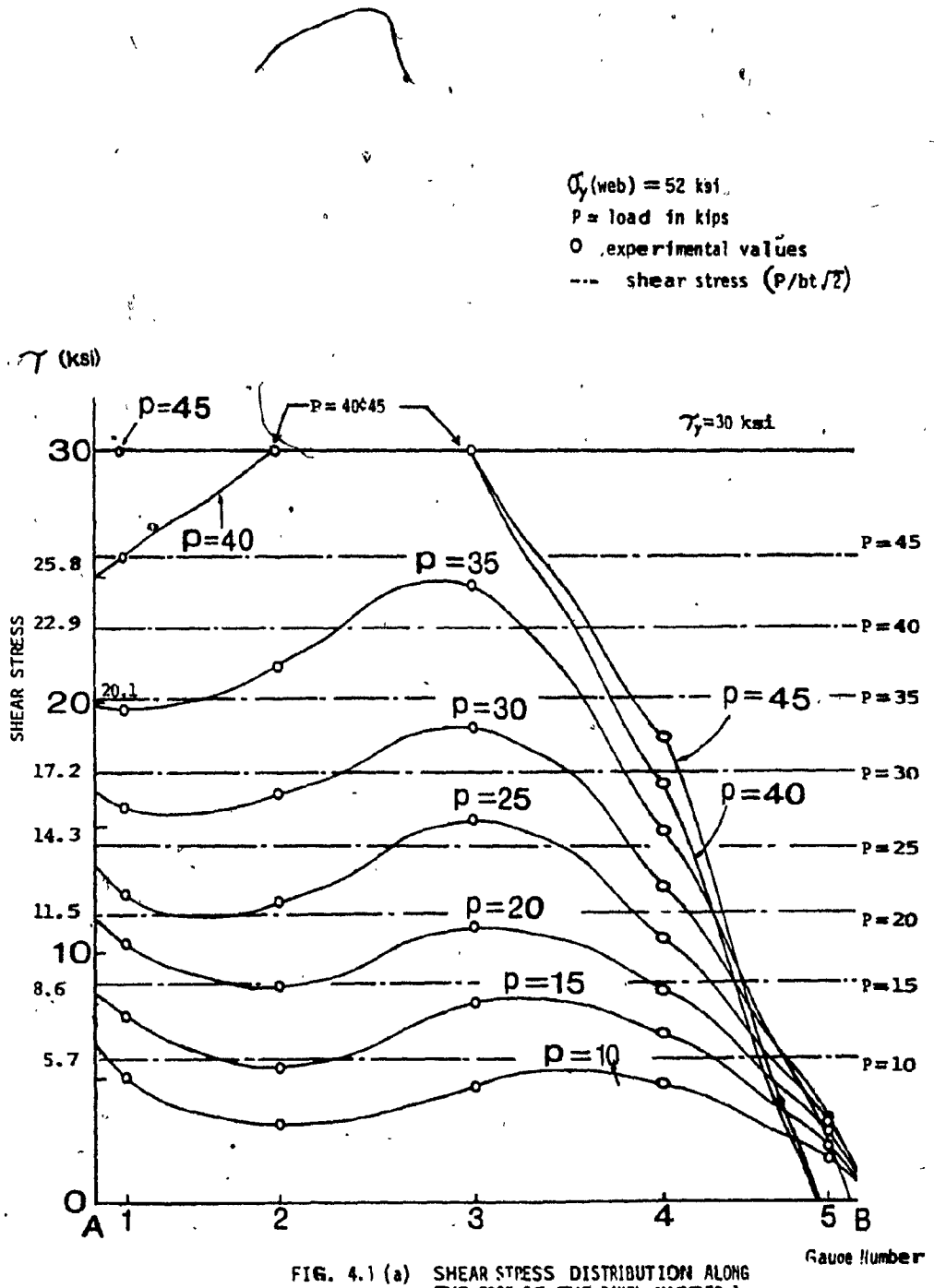

FIG. 4.1 (a) SHEAR STRESS DISTRIBUTION ALONG THE EDGE OF THE PANEL NUMBER 1

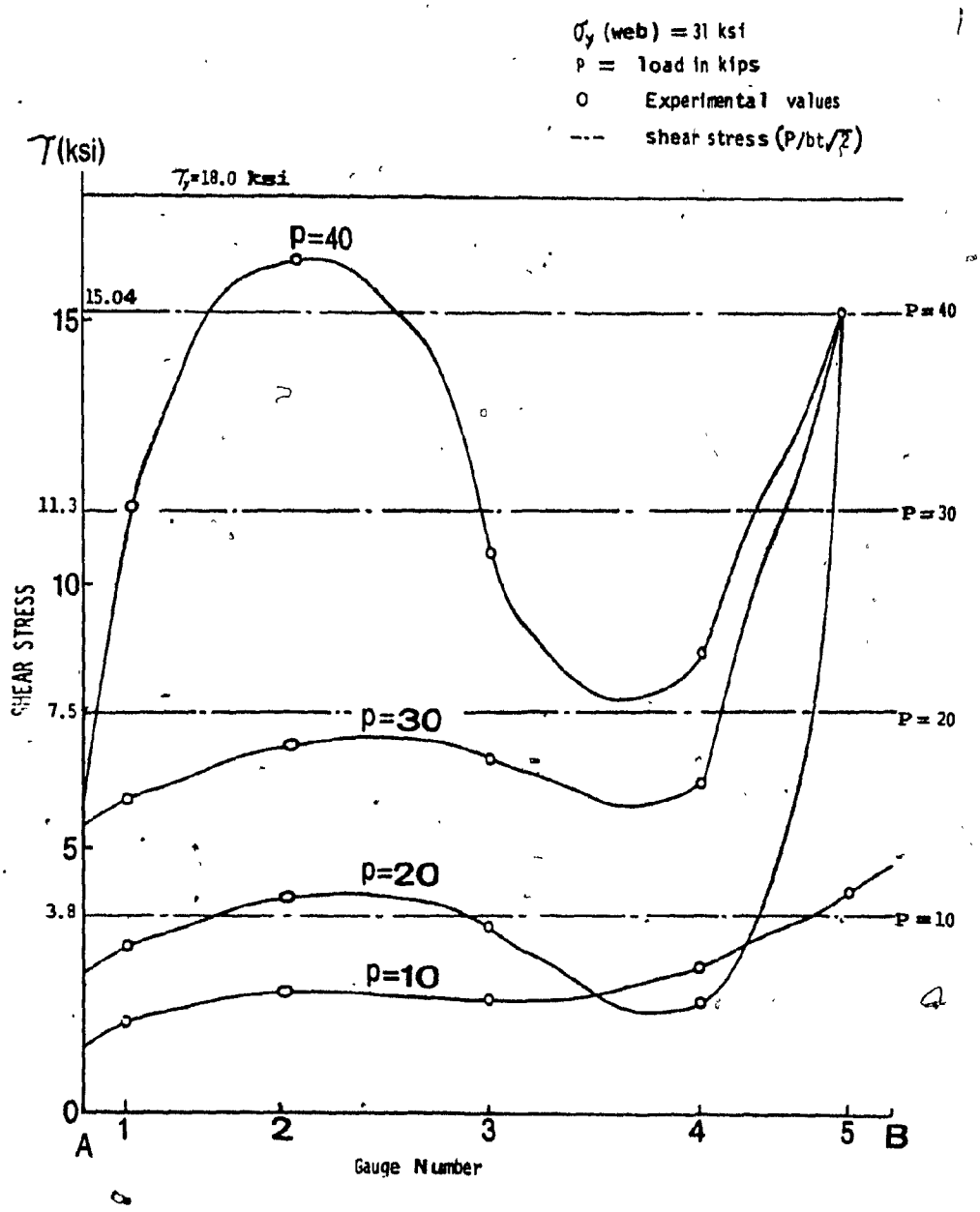

FIG. 4. 1 (b) SHEAR STRESS DISTRIBUTION ALONG THE EDGE OF THE PANEL NUMBER 2

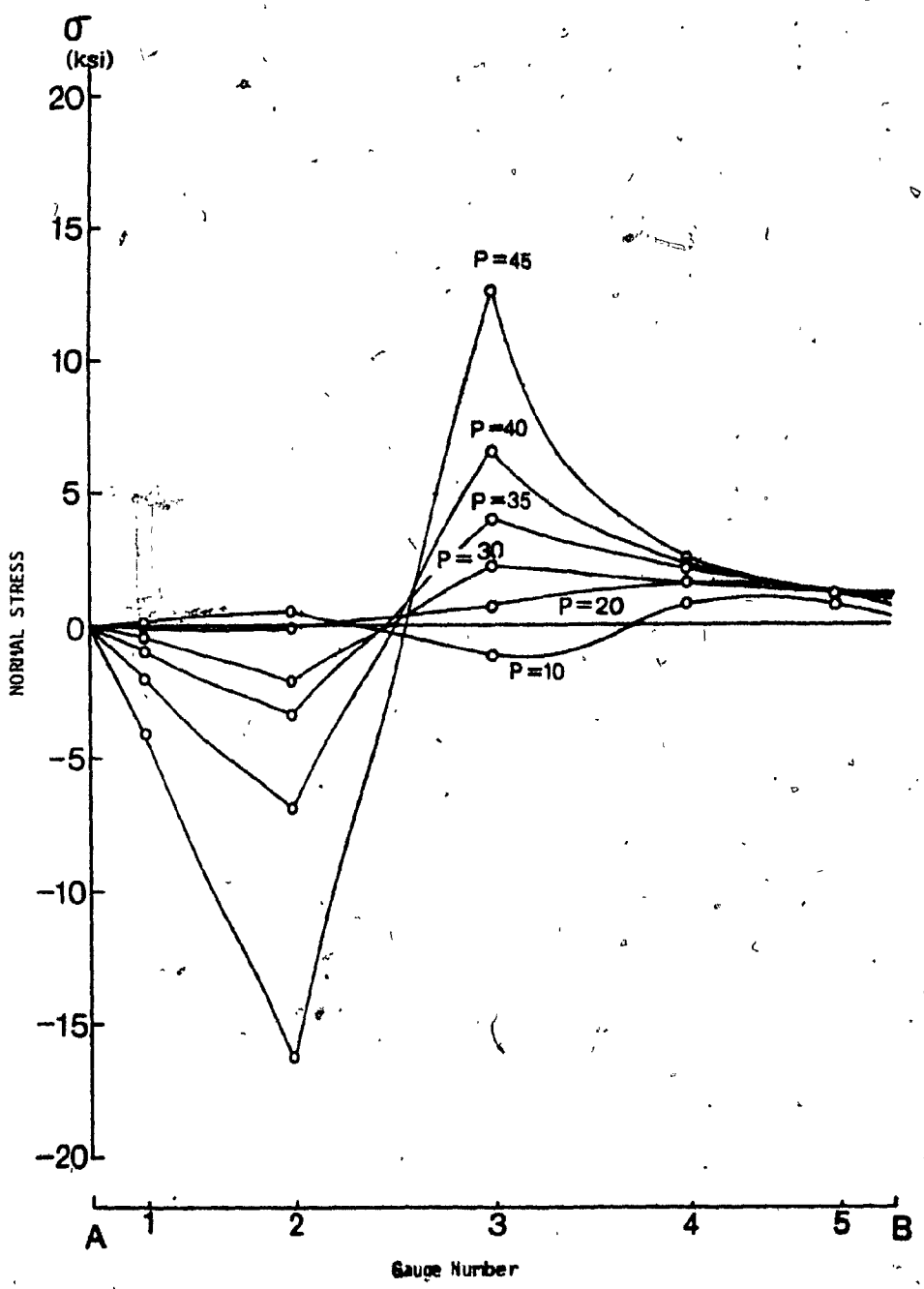

FIG. 4.2(a) NORMAL STRESS DISTRIBUTION ALONG THE EDGE OF THE PANEL NUMBER 1

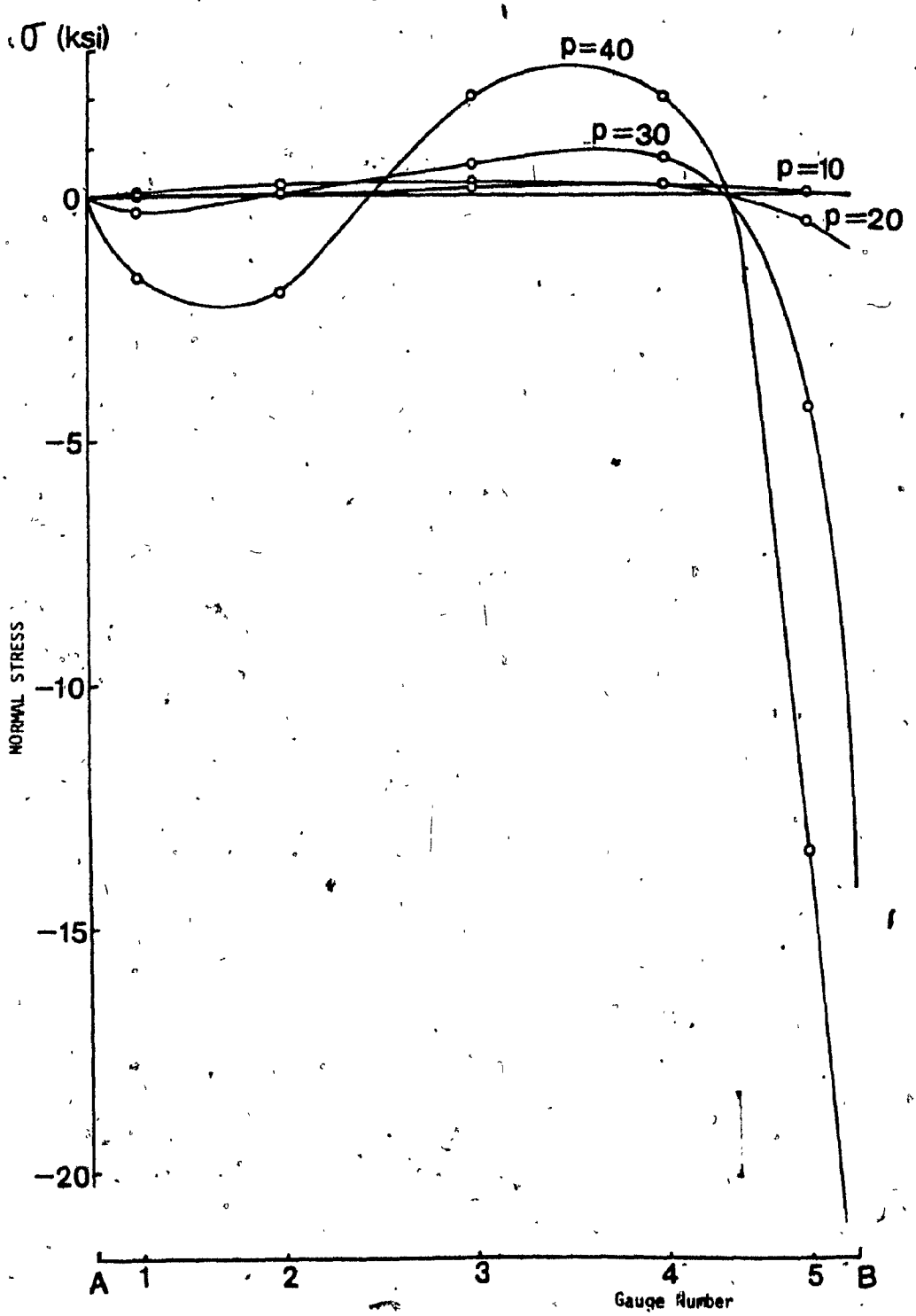

FIG. 4.2 (b) NORMAL STRESS DISTRIBUTION ALONG THE EDGE OF THE PANEL NUMBER 2

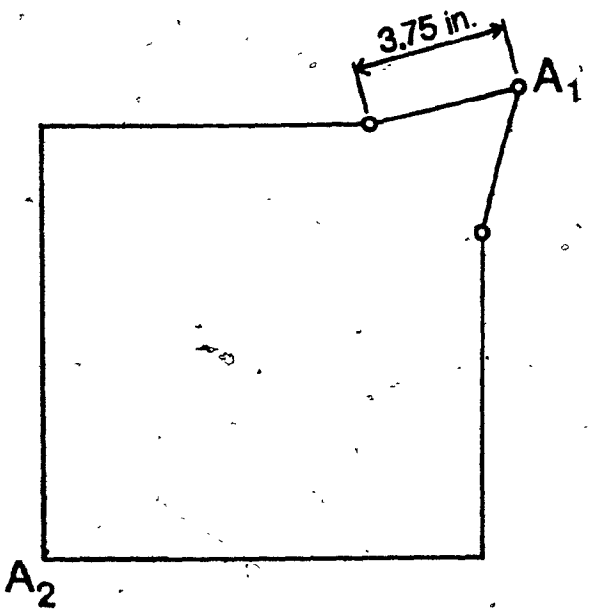

(a). Panel Number 1

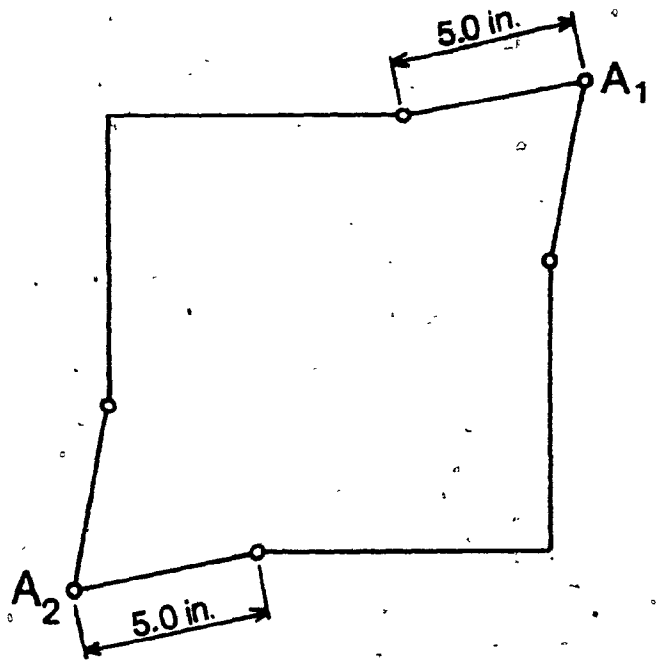

(b) Panel Number 2

FIG. 4.3 COLLAPSE MODES

FIG. 4.4 PANEL NUMBER 1 AT COLLAPSE

FIG. 4.5 PANEL NUMBER 1 AT COLLAPSE

FIG. 4.6 PANEL NUMBER 1 AT COLLAPSE

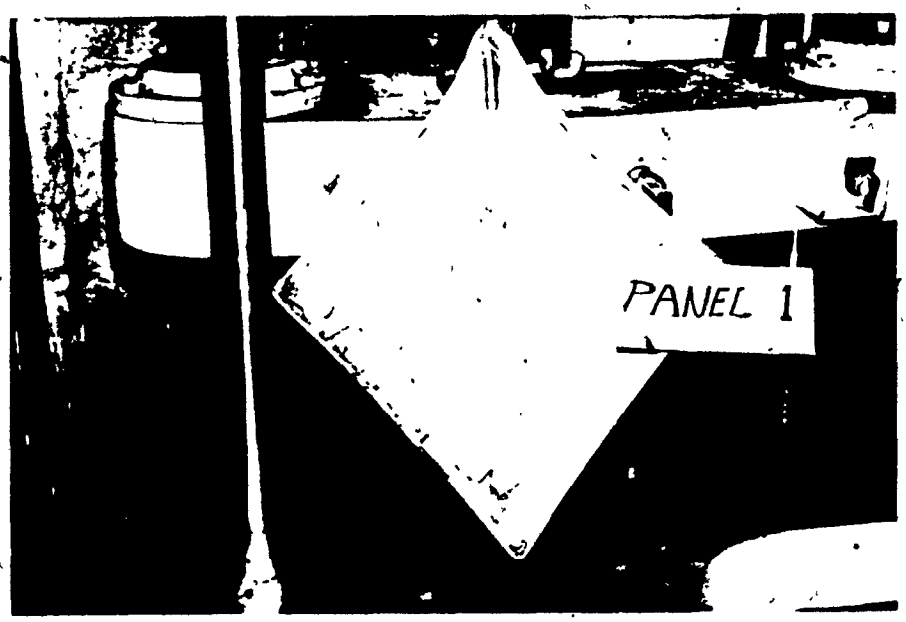

FIG. 4.7 PANEL NUMBER 1 AT COLLAPSE

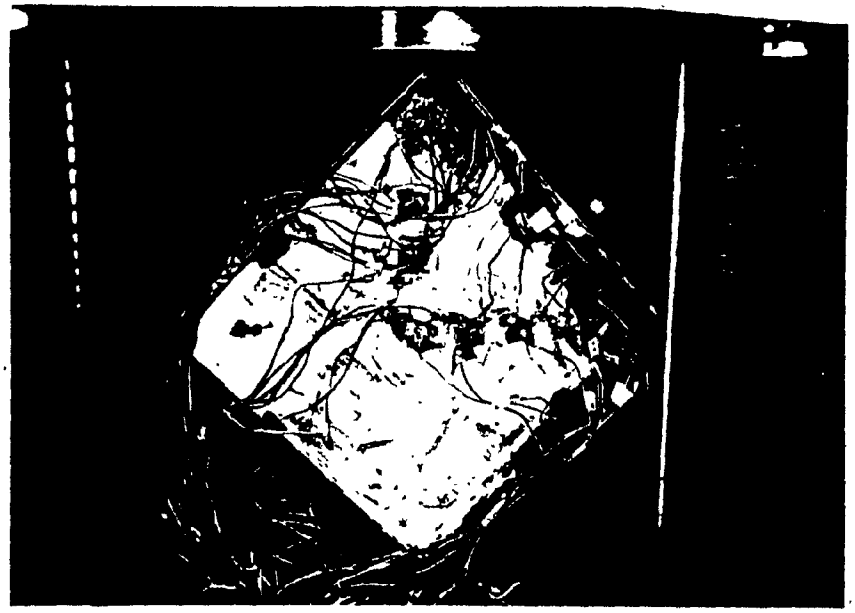

FIG. 4.8 PANEL NUMBER 2 AT BUCKLING

FIG. 4.9 PANEL NUMBER 2 AT COLLAPSE

FIG. 4.10 PANEL NUMBER 2 AT COLLAPSE

Panel No. 1

Load at 10 kips

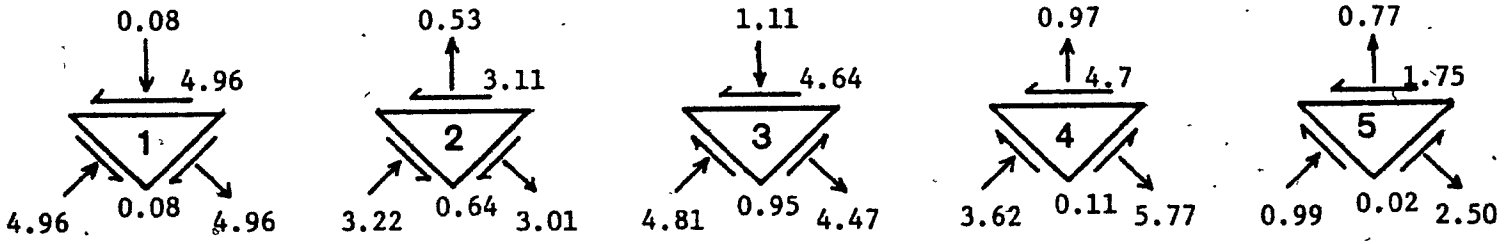

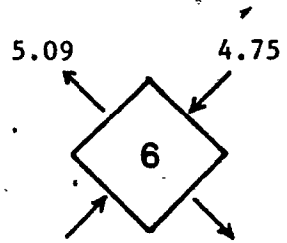

FIG. 4.11 (a) STRESSES ALONG THE EDGE AND AT THE MID POINT OF THE PANEL

Panel No. 1

Load at 15 kips

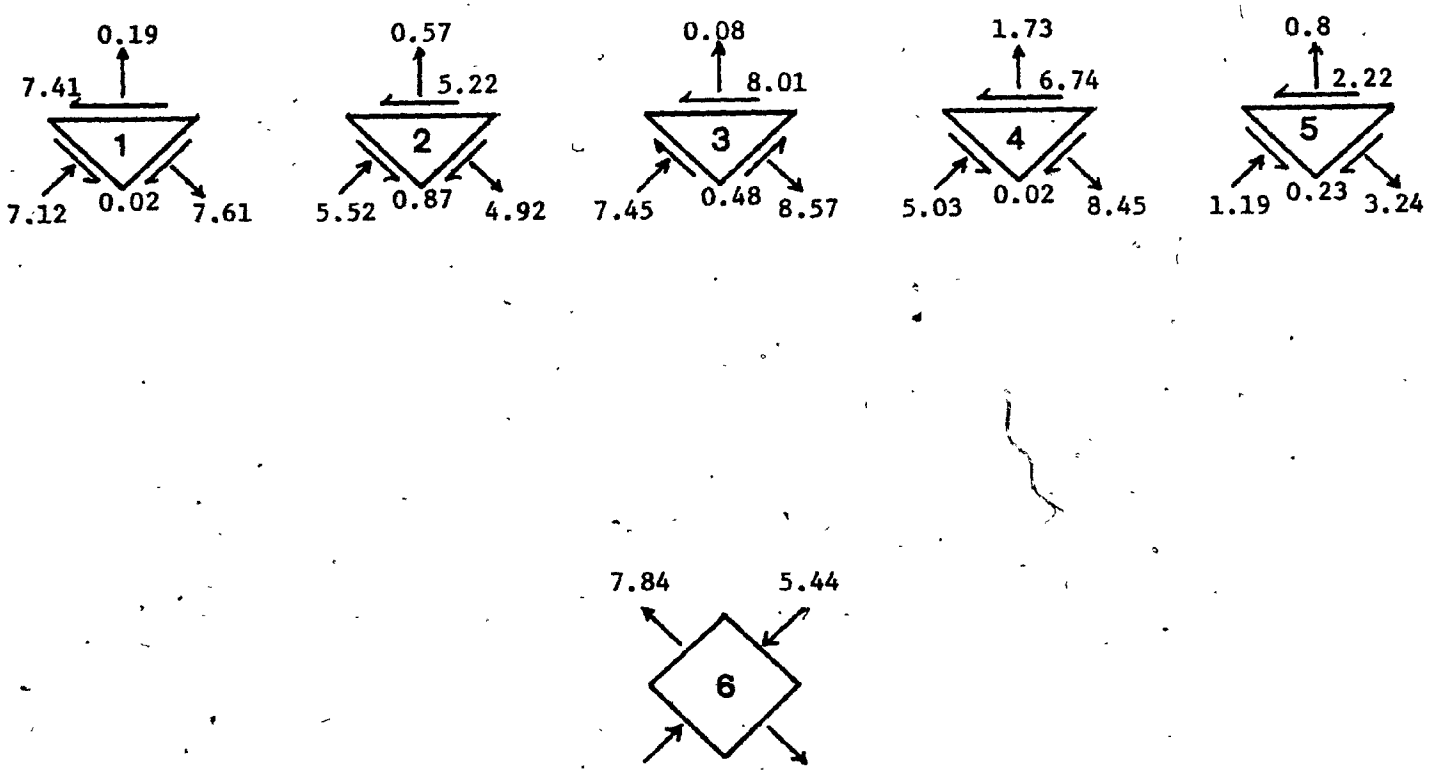

FIG. 4.11 ($_b$) STRESSES ALONG THE EDGE AND AT THE MID POINT OF THE PANEL

Panel No. 1

Load at 20 kips

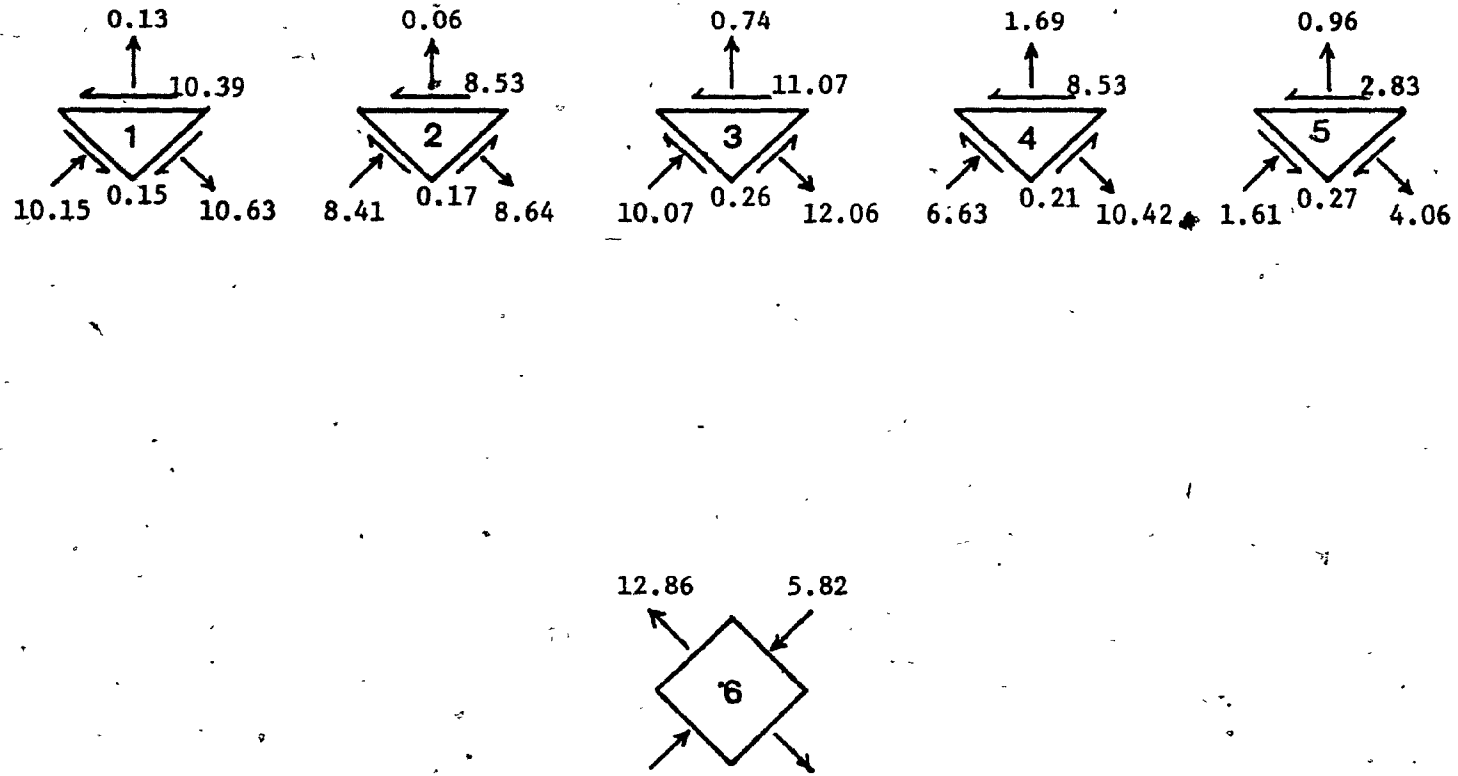

FIG. 4.11 (c) STRESSES ALONG THE EDGE AND AT THE MID POINT OF THE PANEL

Panel No. 1

Load at 25 kips

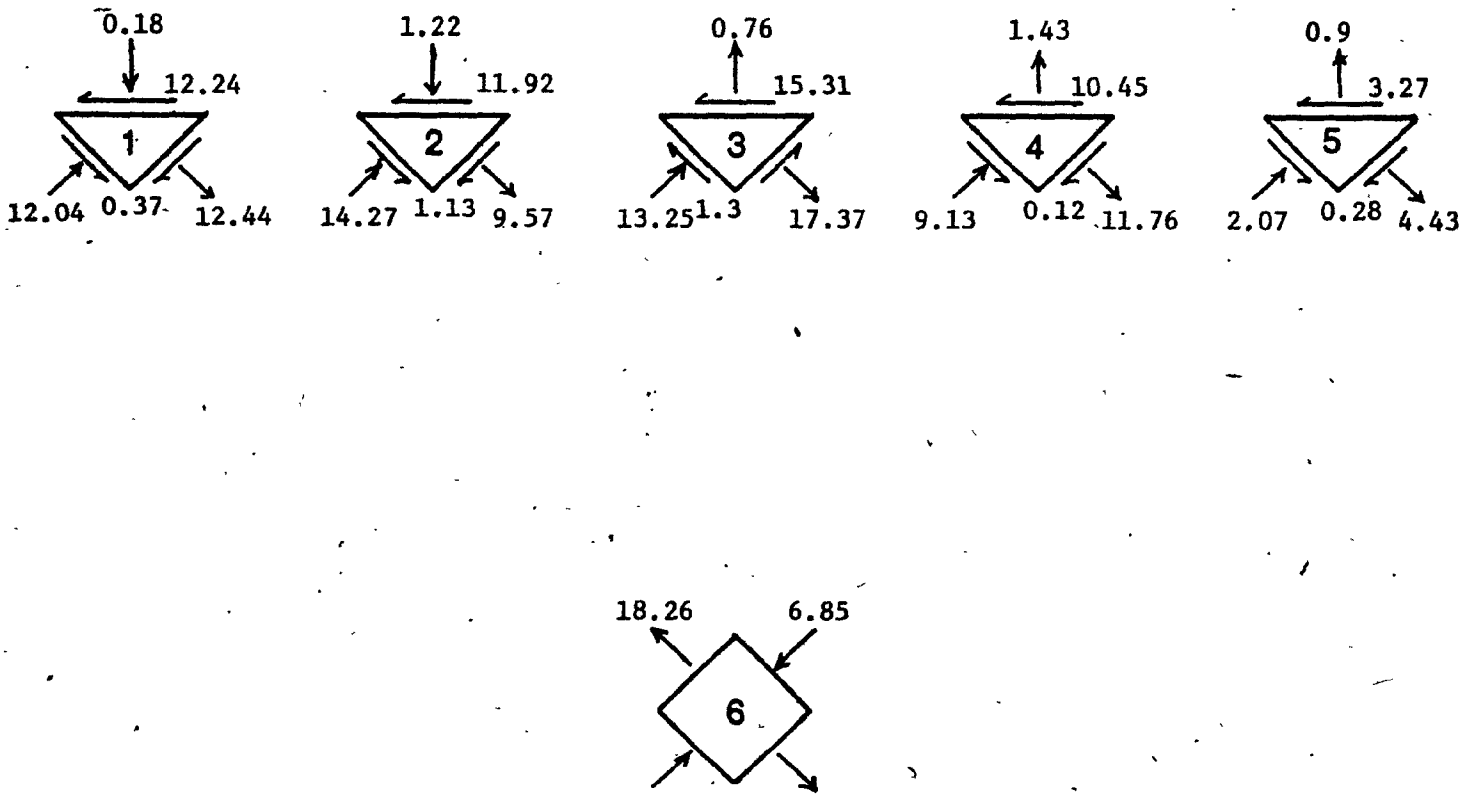

FIG. 4.11 (d) STRESSES ALONG THE EDGE AND AT THE MID POINT OF THE PANEL

Panel No. 1

Load at 30 kips

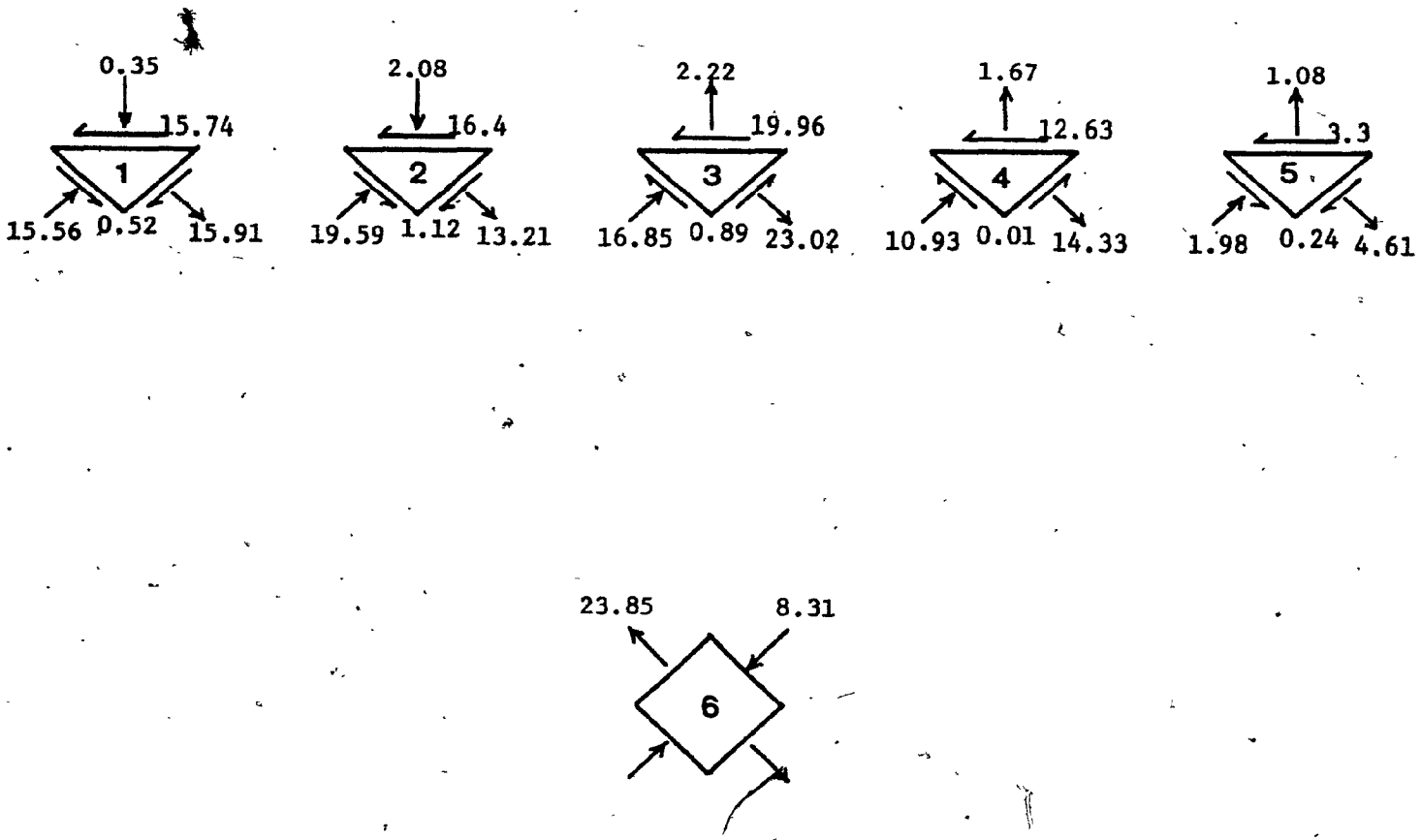

FIG. 4.11 (e) STRESSES ALONG THE EDGE AND AT THE MID POINT OF THE PANEL

Panel No. 1

Load at 35 kips

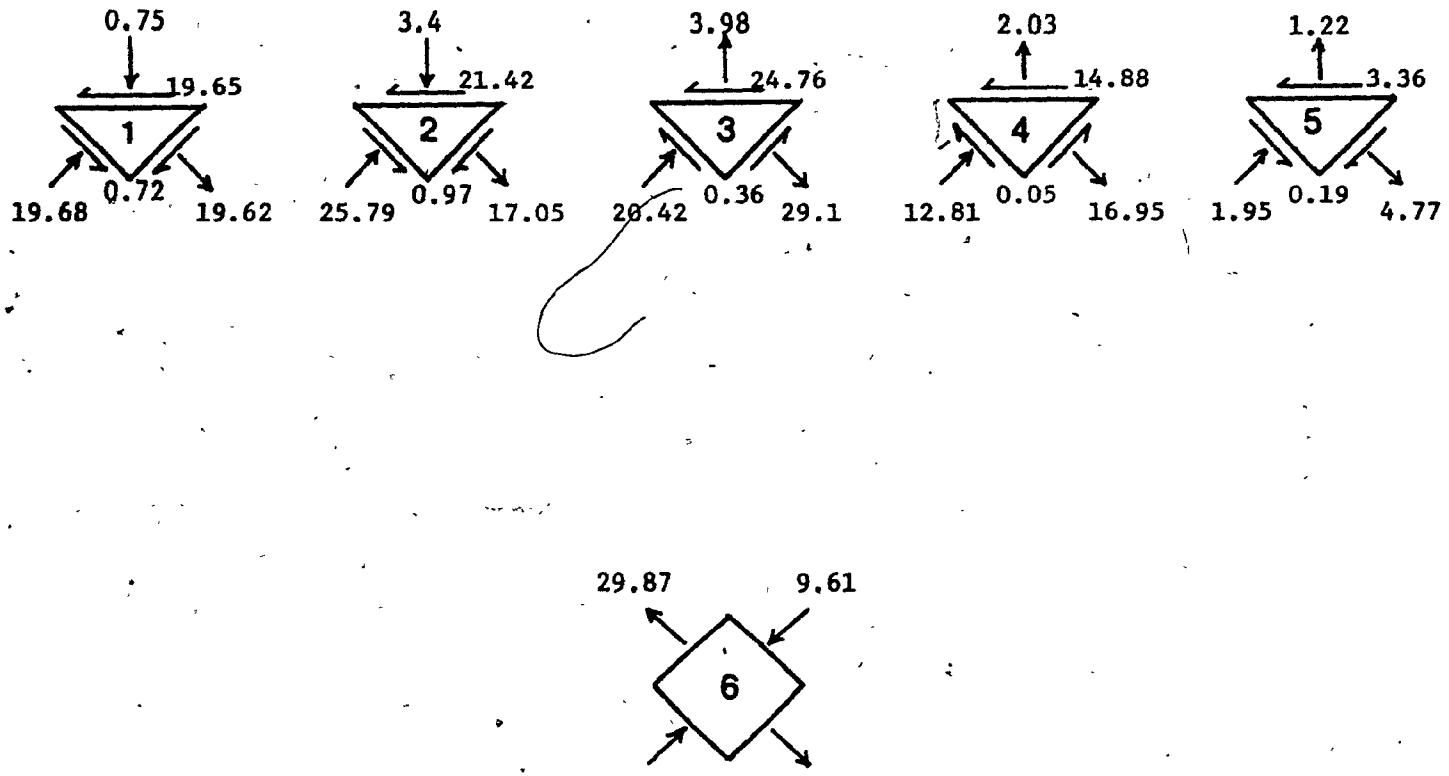

FIG. 4.11 (f) STRESSES ALONG THE EDGE AND AT THE MID POINT OF THE PANEL

Panel No. 1

Load at 40 kips

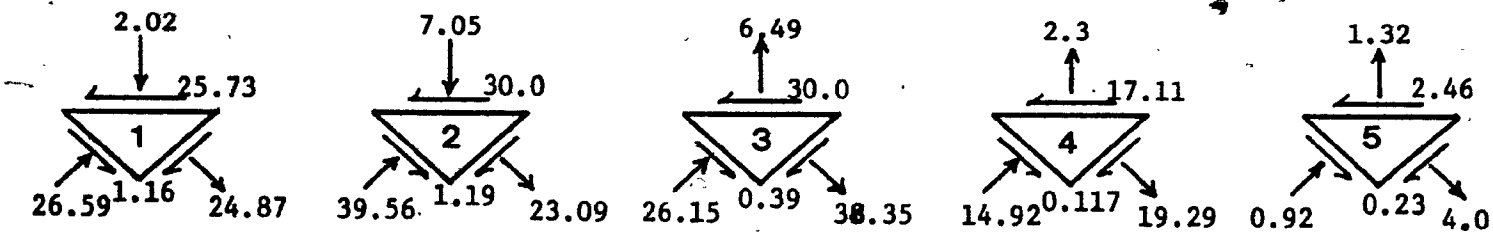

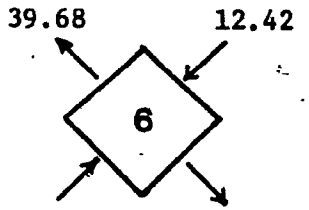

FIG. 4.11 (8) STRESSES ALONG THE EDGE AND AT THE MID POINT OF THE PANEL

Panel No. 1

Load at 45 kips

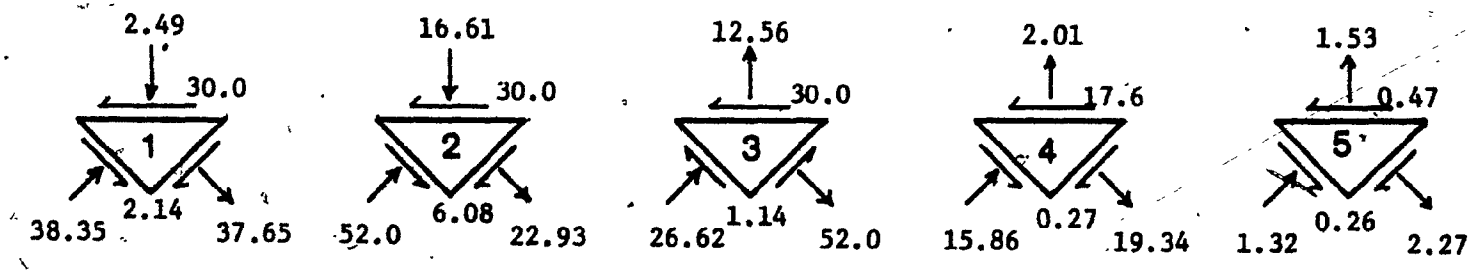

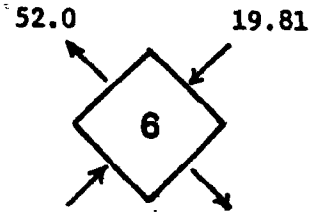

FIG. 4.11 (h) STRESSES ALONG THE EDGE AND AT THE MID POINT OF THE PANEL

Panel No. 2

Load at 10 kips

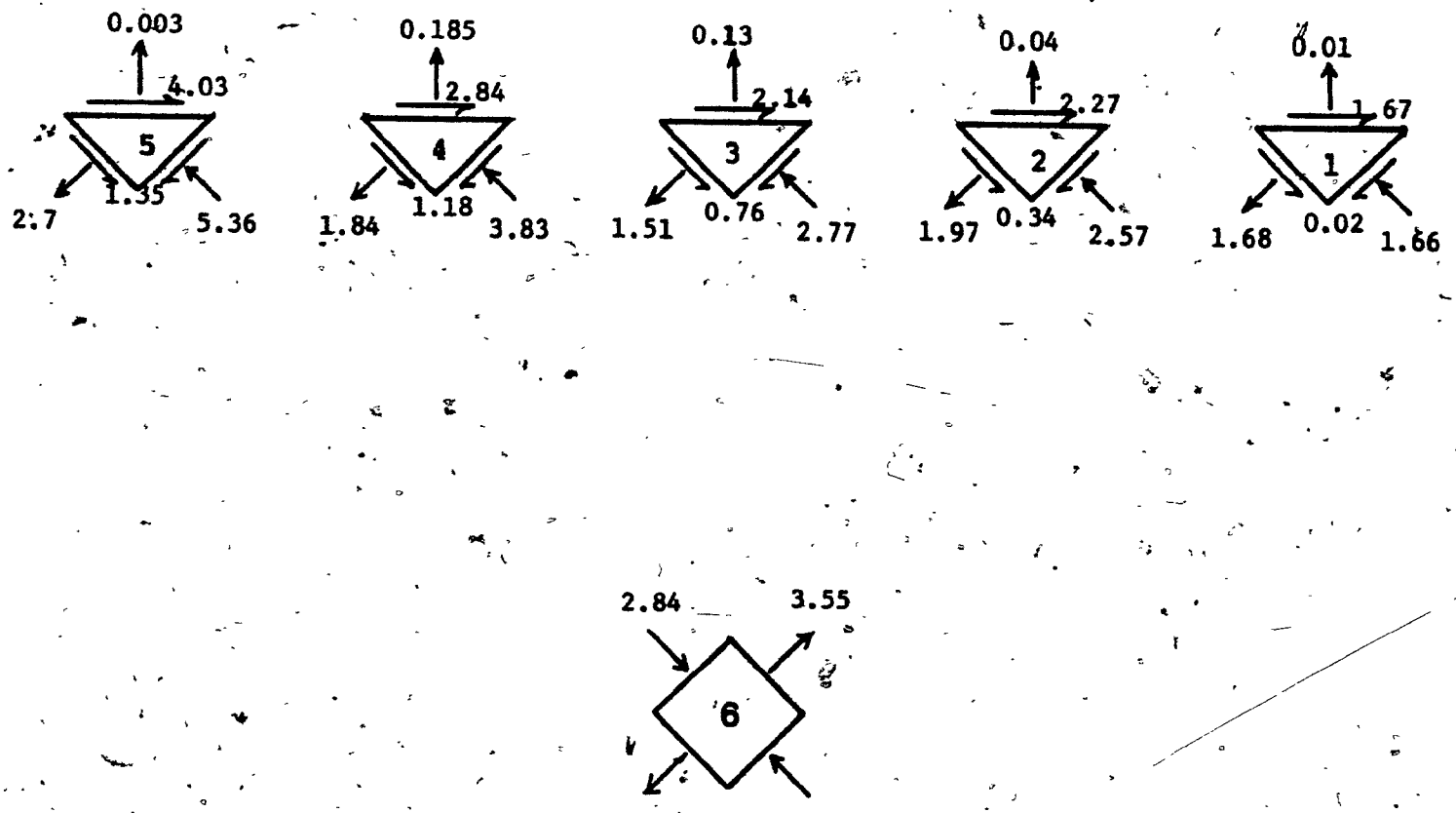

FIG. 4.11 (1) STRESSES ALONG THE EDGE AND AT THE MID POINT OF THE PANEL.

Panel No. 2

Load at 20 kips

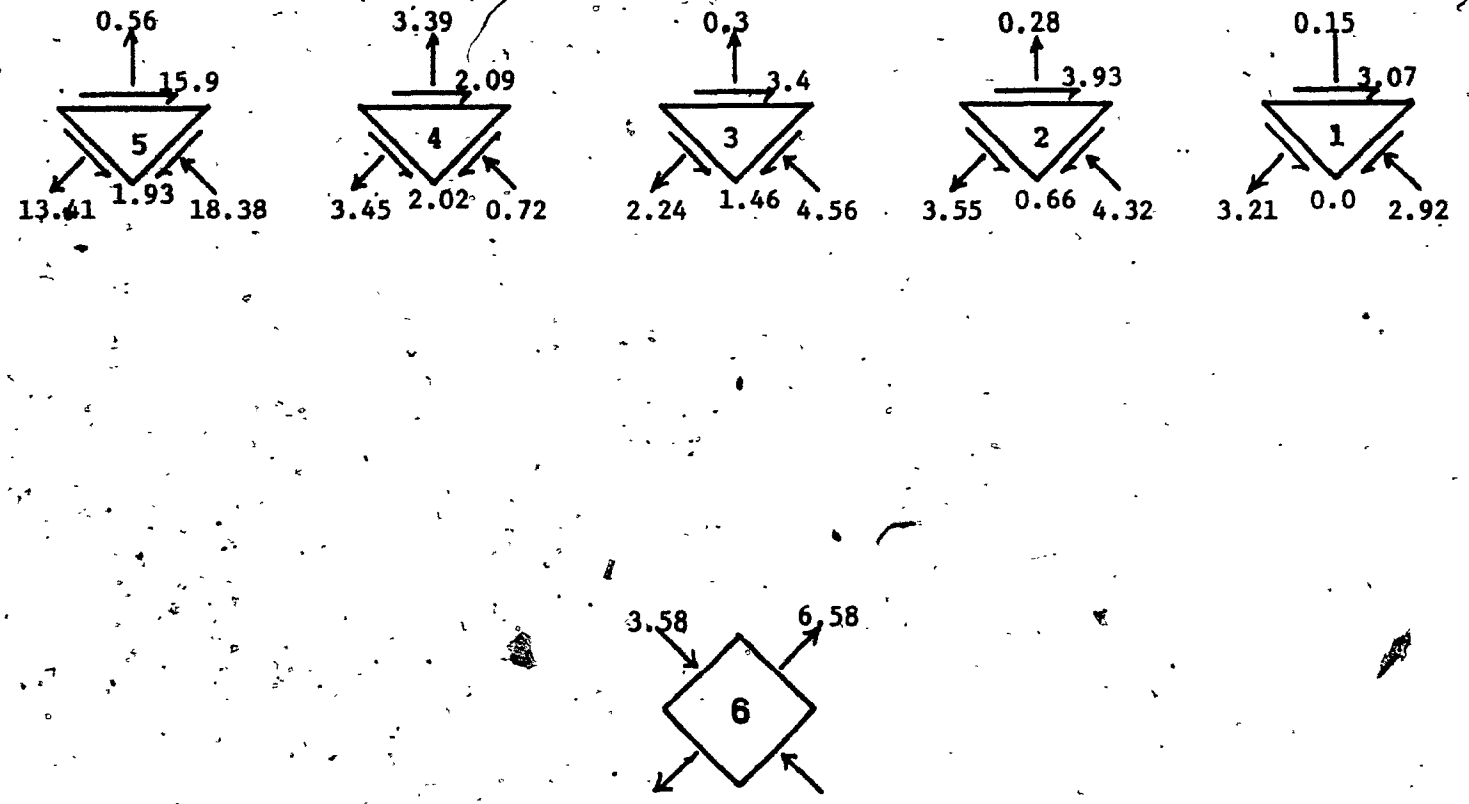

FIG. 4.11 (j) STRESSES ALONG THE EDGE AND AT THE MID POINT OF THE PANEL

Panel No. 2

Load at 30 kips

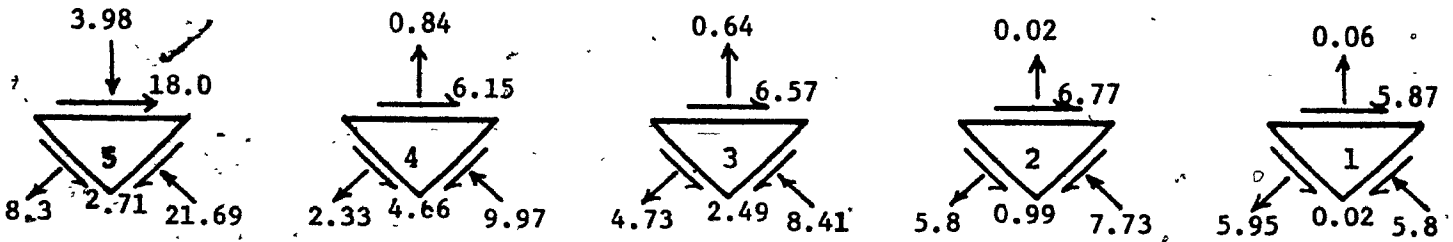

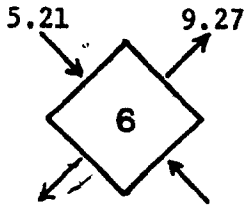

FIG. 4.11 (k) STRESSES ALONG THE EDGE AND AT THE MID POINT OF THE PANEL

Panel No. 2

Load at 40 kips

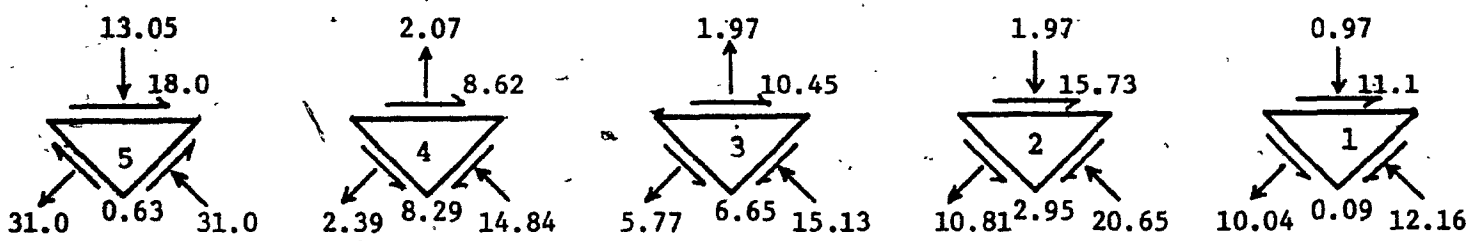

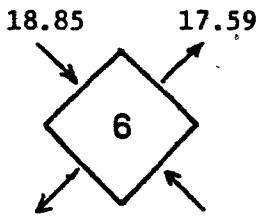

FIG. 4.11 ($_1$) STRESSES ALONG THE EDGE AND AT THE MID POINT OF THE PANEL

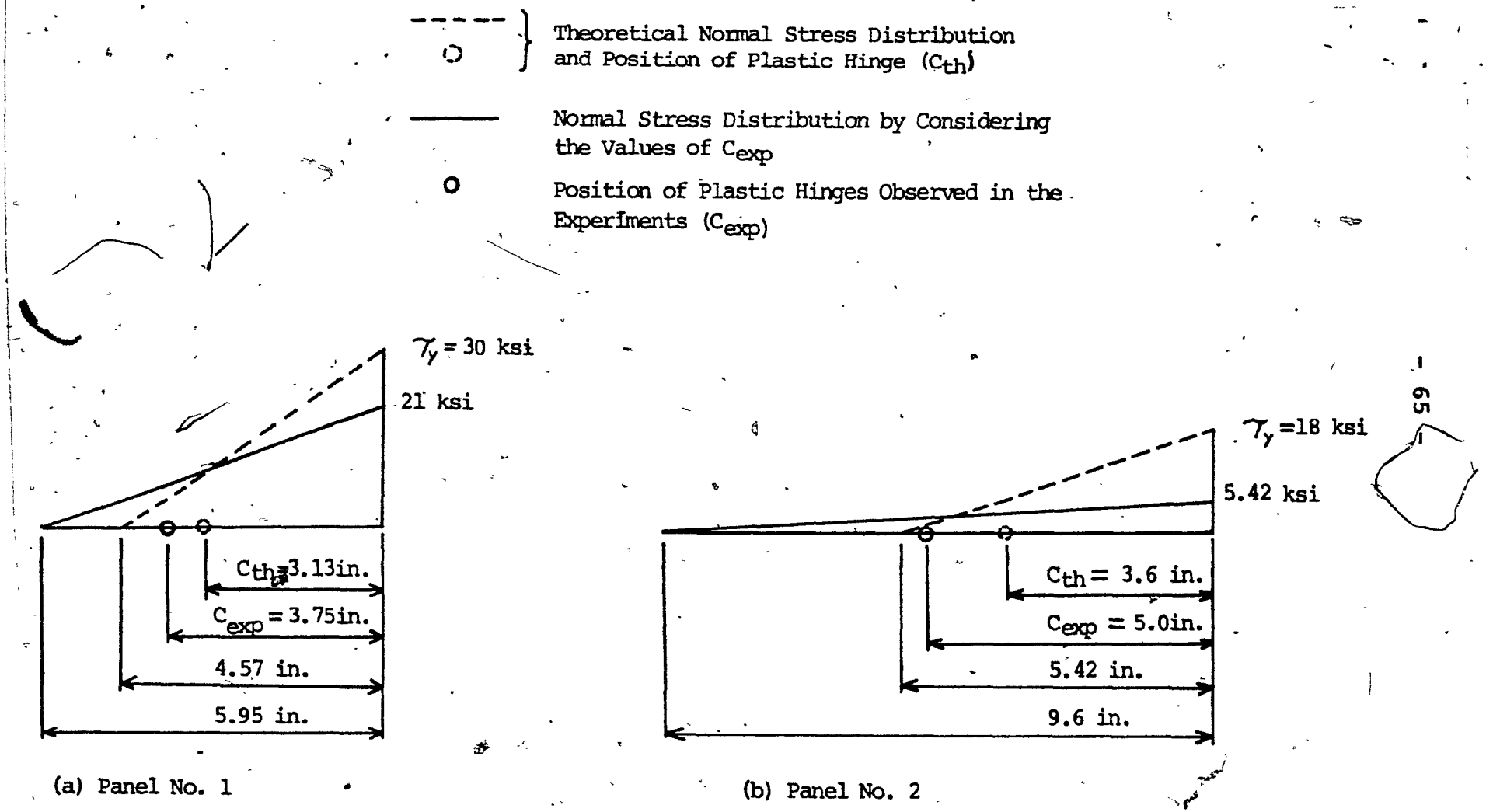

(a) Panel No. 1

(b) Panel No. 2

FIG.4.12 NORMAL STRESS DISTRIBUTIONS AND POSITION OF PLASTIC HINGES
(Refer to Appendix B.2)

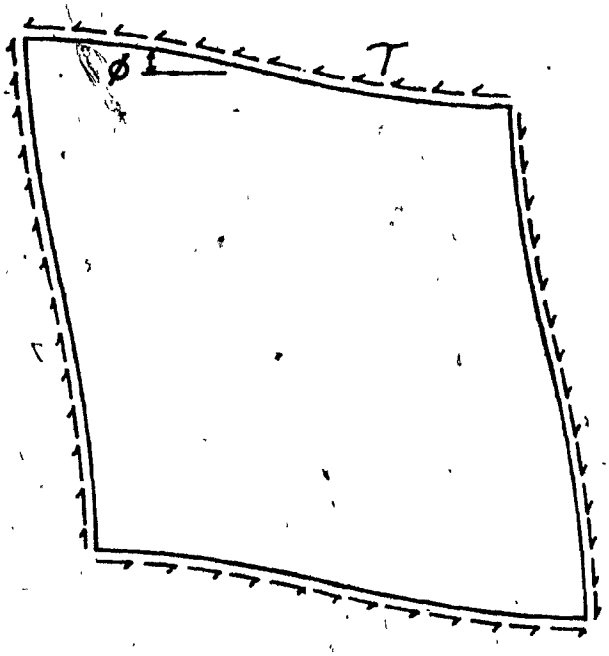

FIG.4.13 DEFORMATION OF A PANEL DUE TO SHEAR STRAIN AND DEFORMATION OF FLANGES

CHAPTER 5

Conclusions and Future Recommendations

CHAPTER 5

Conclusion and Future Recommendations

5.1 Conclusions

Load tests on two single shear panels with different loading systems were conducted. Particular attention was paid to the shear stress distribution along the edge, to see how it compared with the mathematical model proposed in the present theory.

The present study has shown:

1) The shear stress distribution was reasonably uniform at low loading.
2) As the load increases the shear stress became non-uniform with the stress rising more rapidly toward the corner A as predicted.
3) The zero normal stress at the corner A and the self-equilibrating normal stresses along the edge showed that no diagonal tension field was being developed.
4) The secondary normal stress had only a small influence on the behaviour contributing little to the shear capacity.
5) The higher shear stress in test 1 (see Fig. 4.1(a)) at gauge 2 relative to 1 at corner A may have been because of the deformation of the flange due to the loading system. The angle , ϕ, (see Fig. 4.13) represents a rotation due to a shear strain and the deformation of the flange caused by loading system and possibly the shear stress increases as the rotation, ϕ, increases.

6) It was described in the section 4.2.2 that the ultimate shear force of the panel number 1 (Vu = 53 kips) obtained in the experiments was 77% higher than the predicted one (Vu = 30 kips), refering to Table 4.1 while the predicted strength for the panel number 2 was close to the experimental value. The high discrepancy of the ultimate load for the panel 1 is due to the direct transfer of loading across the panel by the loading bracket.

7) Measurement of normal stress was not possible at failure, however the normal stress exerted on the flange by the web at failure, adjacent to the corner to cause yielding in bending of the flange, would have a distribution as shown in Fig. 4.17 (also refer to appendix B.1).

Summarizing the above conclusions:

1) The fundamental shear stress distribution obtained in the experiment approximates one assumed in the theory.

2) No normal stress due to a diagonal tension field was found after the buckling.

3) There were some local influences in the results caused from the manner of loading although it was not critical.

Thus the stress model established in the theory would be quite suitable to use in designing shear panels.

5.2 Future Recommendations

In the experiment on the shear panel the following is to be recommended:

1) The strain should be measured up to the load near the ultimate.
2) A loading system which does not cause high local influence to panels should be prepared.
3) The device (see Fig. 3.7) to measure out-of-plane deformation was not used in the experiment since taking the measurement took too much time. But measurement along one diagonal would provide useful information.

REFERENCES

REFERENCES

(1) "Guide to the Stability Design Criteria for Metal Structure," edited by Bruce G. Johnston, 1976.

(2) Basler, K., "Strength of Plate Girders in Shear," Trans. ASCE, Vol. 128, Part 2 (1963), pp. 683-719.

(3) Basler, K., and Thurlimann, B., "Strength of Plate Girders in Bending," Trans. ASCE, Vol. 128, Part 2 (1963) pp. 655-682.

(4) Basler, K., "Stremgth of Plate Girders Under Combined Bending and Shear," Trans. ASCE, Vol. 128, Part 2 (1963). pp. 720-742.

(5) Rockey, K.C., and Skaloud, M., "The Ultimate Load Behaviour of Plate Girders Loaded in Shear," Struct. Eng., Vol. 50, No. 1 (January 1972, pp. 29-47.

(6) Porter, D.M., Rockey, K.C., and Evans, H.R., "The Collapse Behaviour of Plate Girders Loaded in Shear." Struct. Eng., Vol. 53, No. 8., August 1975, pp. 313-325.

(7) Huslid, J.M., and Rockey, K.C., "The Influence of End Post Rigidity on The Collapse Behaviour," Proc. Instn Civ. Engrs. Part 2, Vol. 67, June 1976, pp. 285-312.

(8) "Strength of Aluminum," Alcan Canada Products Ltd., 1973.

(9) Timoshenko, S.P., and Gere, J.M., "Theory of Elastic Stability," McGraw-Hill, 1961.

(10) Marsh, C., "A Model for the Collapse of Shear Webs," ASCE, Eng. Mech., 1981 (accepted.).

APPENDICES

APPENDIX A

APPENDIX A

The proof of Equations from (12) to (18), given in Chapter 2.

(1) The Proof of Equation 12.

To find the location of the plastic hinge, moment equilibrium at the hinge is used (see Fig. 2.4(a)).

Considering the normal stress and the force, R_1 and R_2, in the stiffeners, for moment equilibrium and $\tau_y = 2\,\tau_y$ (Tresca yield condition),

$$\frac{\tau_{yt}}{2g}(g-e)^3 + \frac{\tau_{yt}}{6g}e^3 = \frac{\tau_{yt}}{2g}e^2(b-g+e)$$

$$+ \frac{2\tau_{yt}}{(2x3g)}(g-e)^3 + \frac{\tau_{yt}}{2g}e(g-e)^2$$

$$\therefore g^3 = 3be^2$$

$$\left(\frac{e}{b}\right)^2 = \frac{1}{3}\left(\frac{g}{3b}\right)^{\frac{1}{2}}$$

$$\therefore \beta' = \alpha\left(\frac{\alpha}{3}\right)^{\frac{1}{2}} \qquad \text{Eq. (12)}$$

APPENDIX

The Proof of The Some Equations in Chapter 2.

(2) The Proof of Equation 13

As can be seen in Fig. 2.4(a), additional shear force, V', is found by the difference of the forces in the two stiffeners, R_1 and R_2, created by the normal stresses.

The additional shear force is,

$$V' = R_2 - R_1 \qquad \text{(A.1)}$$

Substituting the expression of R_1 and R_2 defined in p. 11 into the above equation,

$$V' = \frac{\tau_{yt}}{2} \frac{1}{g}(g^2-e^2-e^2)$$

$$= \frac{\tau_{yt}}{2} g(1-2(\frac{e}{g})^2)$$

$$\therefore \frac{V'}{\tau_y bt} = \frac{\tau'_e}{\tau_y} = \frac{g}{2b}(1-2(\frac{e}{g})^2)$$

$$= \frac{\alpha}{2}(1-2(\frac{1}{g} g(\frac{g}{3b})^{\frac{1}{2}})^2)$$

$$\therefore \frac{\tau'_e}{\tau_y} = \frac{\alpha}{2}(1-\frac{2\alpha}{3}) \qquad \text{Eq. (13)}$$

(3) The Proof of Equation (14)

Considering normal stresses in Fig. 2.4(a) as the static load, the system must be in equilibrium with this load and the plastic moment.

Assuming $q_y = 2\tau_y$, the moment equilibrium is given as follows:

$$\Sigma Mo = \frac{\tau_{yt}}{6}\frac{(g-e)^3}{g} + \frac{yt}{2}\frac{e(g-e)^2}{g}$$

$$= \frac{\tau_{yt}}{6} b^2 \{(\frac{g}{b})^2 - 3(\frac{e}{b})^2(\frac{e}{y})\}$$

$$= \frac{yt}{6} b^2 \{\alpha^2 - 3\frac{\alpha^3}{3} + 2(\frac{\alpha^3}{3})(\frac{\alpha}{3})^{\frac{1}{2}}\}$$

$$= \frac{\tau_{yt} b^2}{6} \alpha^2\{1 - \alpha + \frac{2\alpha}{3}(\frac{\alpha}{3})^{\frac{1}{2}}\}$$

$$\therefore \frac{\Sigma Mo}{\tau_y tb^2} = \mu = \frac{\alpha^2}{6}\{1 - \alpha(1 - \frac{2}{3}(\frac{\alpha}{3})^{\frac{1}{2}}\} \quad \text{Eq. (14)}$$

(4) The Proof of Equation (15)

Relationships between α and β' for finding the position of the plastic hinge is to be found by considering moment equilibrium with respect to the position of the plastic hinge itself.

So $\Sigma M = 0$: with respect to the position of the plastic hinge.

$$\frac{\tau_{yt}}{3g}(e-(g-b))^3 + \frac{\tau_{yt}}{2g}(g-b)(e-(g-b))^2 - \frac{\tau_{yt}}{6g}(g-e)^3$$

$$- \frac{\tau_{yt}}{2g} e(g-e)^2 = 0$$

$$\therefore \left(\frac{e}{b}\right)^2 - \left(\frac{g}{b}\right)^2 + \left(\frac{g}{b}\right) - \frac{1}{3} = 0$$

Letting $\beta = \frac{e}{b}$, $\frac{g}{b} = \alpha$

$$\beta^2 - \alpha(\alpha - 1) - \frac{1}{3} = 0 \text{ ----------(A.2)}$$

Substituting $e = e' + (g - b)$ and letting $\beta' = \frac{e'}{b}$,

$$\left(\frac{e'+g-b}{b}\right)^2 - \alpha^2 + \alpha - \frac{1}{3} = 0$$

$$\therefore \frac{\beta'^2}{2\alpha} + \beta'\left(1 - \frac{1}{\alpha}\right) - \left(\frac{1}{2} - \frac{1}{3\alpha}\right) = 0 \text{ ---------- Eq. (15)}$$

(5) The proof of Eq. (16)

To find the contribution to the shear capacity, first, the forces, R_1 and R_2, in the stiffeners are found from the normal stresses in Fig. 2.4 (b).

$$R_1 = \frac{\tau_{yt}}{2} \frac{1}{g} (e^2 - (b-g)^2 \quad \text{.....(A. 3. a)}$$

$$R_2 = \frac{\tau_{yt}}{2} \frac{1}{g} (g^2 - e^2) \quad \text{.....(A. 3. b)}$$

Then the contribution to the shear capacity is the difference in the forces R_1 and R_1

$$\therefore V' = R_2 - R_1$$

$$= \frac{\tau_{yt}}{2} \frac{1}{g} (2g^2 - 2e^2 + b^2 - 2bg)$$

$$= \frac{\tau_{ytb}}{2} b \left(2 \left(\frac{g}{b}\right)^2 - 2 \left(\frac{e}{b}\right)^2 - 2 \left(\frac{g}{b}\right) + 1\right)$$

$$\therefore \frac{\tau e'}{\tau y} = \frac{v'}{\tau_{ybt}} \frac{1}{2\alpha} (2\alpha^2 - 2\beta^2 - 2\alpha + 1)$$

$$\frac{\tau e'}{\tau y} = \alpha - \frac{\beta^2}{\alpha} + \frac{1}{2\alpha} - 1 \qquad \text{(A. 4)}$$

Substituting $\beta = \{\alpha (\alpha - 1) + 1/3\}$ given by (A. 2) into (A. 4),

$$\frac{\tau e'}{\tau y} = \alpha - \frac{1}{\alpha} (\alpha - \frac{1}{3}) - 1 + \frac{1}{2\alpha}$$

$$\therefore \frac{\tau e'}{\tau y} = \frac{1}{6\alpha} \quad \text{Eq. (16)}$$

(6) Proof of Eq. (17)

Considering the triangular distributed stress (see Fig. 2.4(b)) as a static load, the force in the stiffener, R_1, is

$$R_1 = \frac{g^2 T_y t}{6} - \frac{(g-b)^2}{g} \frac{T_y t}{2} \left(\frac{g-b}{3} + b\right)$$

$$\therefore R_1 = \frac{e'}{g}\left(g - b + \frac{e'}{2}\right) T_y t$$

Taking the moment equilibrium at the plastic hinge where shear is zero,

$$\frac{M_o}{b^2 T_y} = \frac{1}{b^2 t T_y}\left\{R_1 e' - \left(\frac{(g-b+e')^3}{6g} T_y t - \frac{(g-b)^2}{2g}\left(\frac{g-b}{3} + e\right) T_y t\right)\right\}$$

$$\therefore \mu = \left[\left(1-\frac{2}{3\alpha}\right)\beta' - \beta'^2\left(1-\frac{1}{\alpha}\right) - \frac{\beta'^3}{3\alpha}\right] / 4 \quad \ldots\ldots \text{Eq. (17)}$$

APPENDIX B.1

(7) The Proof of Eq. 18

First, relationship between μ and β' is found when the shear stress reaches the yield stress over the entire edge of the panel.

Assuming two plastic hinges as shown in Fig. 2.4,

$$2M_o = \frac{\tau_y(b-e)^2 t}{2} = \frac{\tau_y t}{2}(b^2 - 2be + e^2)$$

$$\frac{4M_o}{\tau_y b^2 t} = 4\mu = 1 - 2\beta + \beta^2$$

$$\beta^2 - 2\beta + 1 - 4M = 0$$

$$\beta = 1 \pm 2\mu^{\frac{1}{2}} \qquad (A.5)$$

then its shear contribution is,

$$V' = R_2 - R_1 = (b-e')\tau_y t - e'\tau_y t$$

$$= \tau_y t(b - 2e') \qquad (A.6)$$

$$\frac{\tau e}{\tau_y} = 1 - 2\beta$$

substituting (A.5) into (A.6),

$$\frac{\tau e}{\tau_y} = 1 - 2(1 \pm 2\mu^{\frac{1}{2}})$$

$$\therefore \frac{\tau e}{\tau_y} = 4\mu^{\frac{1}{2}} - 1 \qquad \text{Eq. (18)}$$

APPENDIX B.1

Theoretical Shear Strength

(1) Panel No. 1: $\tau_{yf} = 58$ ksi; $\tau_y = 52$ ksi

According to the theory developed in Chapt. 2, it is as follows:

Plastic Moment, Mo, is,

$$Mo = \frac{b_f t_f^2 \tau_{yf}}{4} = 3.54 \text{ kips - in}$$

The value of μ is,

$$\mu = \frac{Mo}{b^2 t \tau_y}$$

$$= \frac{3.54}{15.23^2 \times 0.081 \times 30}$$

$\therefore \mu = 0.0063$

Then from Fig. 2.7,

$\alpha = 0.3$

Since $\alpha < (\tau o/\tau y)^{\frac{1}{2}} = 0.44$, refering to Table 2.1

$$\frac{\tau_e}{\tau_y} = 2\left(\frac{\tau_o}{\tau_y}\right)^{\frac{1}{2}} + \frac{\tau_o}{\tau_y}$$

$\tau_e = 20.52$ ksi

The shear force due to the contribution of the web is,

$$V_e = \tau_e bt$$

$$= 25.31 \text{ kips}$$

The additional shear force, V_e', due to the strength of the flange is,

$$\frac{\tau_e'}{\tau_y} = \frac{\alpha}{2}\left(1-\frac{2\alpha}{3}\right)$$

$$\tau_e' = 3.6 \text{ ksi}$$

$$V_e' = \tau_e' bt$$

$$= 4.44 \text{ kips}$$

Thus the shear strength of the panel is

$$V_u = V_e + V_e'$$

$$= 29.85 \text{ kips}$$

(2) Panel No. 2: $\tau_{yf} = 48.94$ ksi

$\tau_y = 32$ ksi

Follow the same steps used in (1)

(a) Shear Strength:

Plastic moment is considered as

$$Mo = \frac{M_1 + M_2}{2}$$

where: $M_i = \frac{b_f t_f^2 \tau_{yf}}{4}$, a plastic moment at the corner,

$M_2 = \frac{t_f \tau_{yf}}{4}$ (b_f - size of two holes), a plastic moment at bolt holes and size of one bolt hole = 0.67 in.

$$Mo = \frac{1}{2}(5.17 + 3.42)$$

$$= 4.3 \text{ kips - in.}$$

$\therefore \mu = 0.0082$

$\alpha = 0.36 < \left(\frac{\tau_o}{\tau_y}\right)^{\frac{1}{2}}$

Refering to Table 2.1, the shear force, V_e is,

$$\frac{\tau_e}{\tau_y} = 0.983$$

$\therefore V_e = 0.983 \tau_y bt$

$= 33.29$ kips

The additional shear force, V_e' is,

$$\frac{\tau_e'}{\tau_y} = 0.137$$

$$\therefore V_e = 4.64 \text{ kips}$$

Thus the shear strength of the panel is

$$\therefore V_u = V_e + V_e'$$

$$= 37.93 \text{ kips}$$

APPENDIX B.2

Appendix B.2

Normal Stress Distributions (the one defined theoretically and the other defined by considering the position of the plastic hinges in the experiments)

(1) Panel No. 1

(i) Using the value of α defined in Appendix B.1 and eq. (12) theoretically,

$$g = \alpha \cdot b$$
$$= 4.57 \text{ in}$$
$$\frac{e}{b} = \alpha \left(\frac{\alpha}{3}\right)^{\frac{1}{2}}$$
$$= 0.095$$
$$e = 1.44 \text{ in.}$$
$$c = g - e$$
$$= 3.13 \text{ in (a position of the plastic hinge)}$$

(ii) Refering to Eq. (12),

$$g^3 = 3be^2 = 3b(g-c)^2$$

Substituting C = 3.75 in, the position of the plastic hinge obtained in the experiment, into the above equation,

$g = 5.95$ in. ($\alpha = g/b = 0.39$)

Then Eq. (14) for the case of two plastic hinges (i.e., $\Sigma Mo = 2Mo$) gives:

$$\mu = \frac{2Mo}{b^2 t \tau} = 0.009 \quad \text{where } \tau \neq \tau_y$$

Considering Mo = 3.54 kips - in as defined in Appendix B.1,

τ = 21. ksi (maximum stress at the corner instead of σ_y)

This normal stress distribution is shown in Fig. 4.12 (a).

(2) Panel No. 2

(i) $g = \alpha \cdot b$

$= 0.35 \times 15.05$

$= 5.42$ in.

$\frac{e}{b} = 0.12$

$\therefore e = 1.87$ in.

$\therefore c = g - e = 3.6$ in.

(ii) Using Eq. (12) and C = 5 in, the position of the plastic hinge occured at the bolt,

$g^3 = 3b(g-c)^2$

$g = 9.6$ in

Substituting $\alpha = g/b = 0.636$ into Eq. (14),

$\mu = 0.026$

$\therefore \tau = 5.8$ ksi (maximum stress at the corner instead of σ_y)

This normal stress distribution is shown in Fig. 4.12 (b).